

# Scores Know Bob's Voice: Speaker Impersonation Attack

Chanwoo Hwang\*  
Hanyang University  
Seoul, Republic of Korea  
aa5568@hanyang.ac.kr

Sunpill Kim\*  
Hanyang University  
Seoul, Republic of Korea  
ksp0352@gmail.com

Yong Kiam Tan<sup>†‡</sup>  
I<sup>2</sup>R, A\*STAR & NTU  
Singapore  
yongkiam.tan@ntu.edu.sg

Tianchi Liu  
National University of Singapore  
Singapore  
tianchi\_liu@u.nus.edu

Seunghun Paik\*  
Hanyang University  
Seoul, Republic of Korea  
whitesoonguh@hanyang.ac.kr

Dongsoo Kim\*  
Hanyang University  
Seoul, Republic of Korea  
frds37@hanyang.ac.kr

Mondal Soumik<sup>†</sup>  
I<sup>2</sup>R, A\*STAR  
Singapore  
Soumik\_Mondal@a-star.edu.sg

Khin Mi Mi Aung<sup>†</sup>  
I<sup>2</sup>R, A\*STAR  
Singapore  
Mi\_Mi\_Aung@a-star.edu.sg

Jae Hong Seo<sup>§</sup>  
Hanyang University  
Seoul, Republic of Korea  
jaehongseo@hanyang.ac.kr

## Abstract

Advances in deep learning have enabled the widespread deployment of speaker recognition systems (SRSs), yet they remain vulnerable to score-based impersonation attacks. However, existing attacks operating on raw waveforms require a large number of queries, stemming from the inherent difficulty of performing optimization over high-dimensional audio spaces. Optimization within the latent space of generative models presents a compelling alternative to improve efficiency, yet a fundamental mismatch exists: these latent spaces are typically shaped by data distribution matching, which does not inherently capture the speaker-discriminative geometry. Consequently, optimization trajectories in the latent space often fail to align with the adversarial direction required to maximize the score with the victim.

To resolve this, we propose an inversion-based generative attack framework that explicitly aligns the latent space of the synthesis model with the discriminative feature space. We first analyze the requirements for an *inverse model* to facilitate score-based attacks. Guided by this, we introduce a training strategy enforcing feature-aligned inversion, which geometrically synchronizes the latent inputs with the feature space of SRSs. This synchronization ensures that updates in the latent space translate directly into improvements in attack scores. Furthermore, this capability enables

emerging attack paradigms—such as subspace-projection-based attacks—which were previously inapplicable to SRSs due to the lack of a faithful mapping between features and audio.

Experiments demonstrate that our approach achieves superior query efficiency compared to baselines, attaining competitive attack success rates with on average 10× fewer queries. In particular, the enabled subspace-projection-based attack achieves a high success rate of up to 91.65% using only 50 queries, validating the efficacy of the proposed alignment. These results establish feature-aligned inversion as a crucial instrument for assessing the robustness of modern SRSs against score-based impersonation threats.

## CCS Concepts

• Security and privacy → Biometrics.

## Keywords

Speaker Recognition; Impersonation Attack; Black-box Attack; Score Query based Attack.

## ACM Reference Format:

Chanwoo Hwang, Sunpill Kim, Yong Kiam Tan, Tianchi Liu, Seunghun Paik, Dongsoo Kim, Mondal Soumik, Khin Mi Mi Aung, and Jae Hong Seo. 2018. Scores Know Bob's Voice: Speaker Impersonation Attack. In *Proceedings of Make sure to enter the correct conference title from your rights confirmation email (Conference acronym 'XX)*. ACM, New York, NY, USA, 27 pages. <https://doi.org/XXXXXXXX.XXXXXXX>

## 1 Introduction

Speaker recognition systems (SRSs) aim to verify or identify individuals based on their voice characteristics [5]. Recent advances in deep learning have led to their widespread deployment in security-critical applications such as biometric authentication, forensics, and voice-controlled services [44, 76]. In response, their security has attracted growing attention, and a key security threat to SRSs is *speaker impersonation* where an adversary attempts to be accepted by the system as a specific enrolled identity.

A wide range of attacks against SRSs have been studied under different settings, including human voice mimicry [37], replay attacks [84], adversarial attacks [9, 10, 20, 85, 87], and speech

\*Department of Mathematics & Research Institute for Natural Sciences

<sup>†</sup>I<sup>2</sup>R: Institute for Infocomm Research, A\*STAR

<sup>‡</sup>NTU: Nanyang Technological University

<sup>§</sup>Corresponding Author

Permission to make digital or hard copies of all or part of this work for personal or classroom use is granted without fee provided that copies are not made or distributed for profit or commercial advantage and that copies bear this notice and the full citation on the first page. Copyrights for components of this work owned by others than the author(s) must be honored. Abstracting with credit is permitted. To copy otherwise, or republish, to post on servers or to redistribute to lists, requires prior specific permission and/or a fee. Request permissions from [permissions@acm.org](mailto:permissions@acm.org).  
*Conference acronym 'XX, Woodstock, NY*

© 2018 Copyright held by the owner/author(s). Publication rights licensed to ACM.  
ACM ISBN 978-1-4503-XXXX-X/18/06  
<https://doi.org/XXXXXXXX.XXXXXXX>

synthesis-based approaches [30, 46]. These attacks are typically investigated under different threat models and are not always explicitly framed as impersonation attacks. Nevertheless, they share a common functional outcome: generating audio that is accepted by the system as a specific enrolled speaker. From this perspective, we collectively refer to such attacks as *speaker impersonation*.

Most existing impersonation attacks, however, assume that the adversary has access to the victim’s voice samples. While such works help understand security risks under strong adversarial assumptions, access to a victim’s voice samples cannot always be justified in practical deployments due to strict privacy regulations [71] and standards [29]. They prohibit the storage and distribution of raw biometric data, and enrolled identities are often represented only through templates rather than stored speech signals. In such scenarios, an adversary may know that a target identity is enrolled in the system, yet lack access to any corresponding voice recordings.

Under such a constraint, an alternative attack surface arises: the *score-based black-box setting*. In this setting, the adversary interacts with the SRS solely through similarity scores and has no access to the victim’s voice samples. This threat model surface is motivated by a typical system’s verification process in practical SRSs. They often provide similarity scores, either explicitly to support flexible decision policies or implicitly as part of their internal decision mechanism.[4, 48, 56] These scores quantify how closely a given input matches an enrolled identity and thus constitute a potential source of information for impersonation attempts.

Despite the real-world relevance of this threat model, speaker impersonation attacks under this setting have received relatively limited attention, in contrast to other biometric domains, e.g., face [36, 64, 70], finger vein [52], fingerprints [6]. To our knowledge, FakeBob [9] represents one of the few attempts to perform speaker impersonation using score-based feedback only. While FakeBob proposed a zeroth-order optimization strategy from gradient estimation to iteratively modify the input audio signal, their attack requires a prohibitively large number of score queries. This inefficiency arises because direct optimization in the raw audio space introduces a severe mismatch between the search space and the speaker-discriminative representation used by the recognition system. This observation raises a fundamental research question: *Is direct optimization in the audio domain the most appropriate way to formulate score-based speaker impersonation attacks?*

## 1.1 Observation: Search Space Misalignment

To address the question, we revisit score-based attacks through the lens of black-box optimization, identifying the key bottleneck as the misalignment between the search space and the scoring objective.

**Formulating Score-based Attacks.** Fundamentally, the adversarial goal of score-based impersonation attacks is to find an audio signal whose similarity score with the target identity exceeds a decision threshold. By viewing the similarity score as the objective, we can reformulate these attacks in terms of a black-box optimization problem to maximize the score. This formalization generalizes FakeBob as it utilizes an NES-based [78] optimizer to solve this problem, leveraging raw audio space as the search space.

While this formulation is general, its practical effectiveness depends critically on the choice of the search space in which optimization is performed. As observed by FakeBob, direct optimization in the raw audio space is prohibitively inefficient due to its extremely high dimensionality; the effectiveness of the NES solver is known to degrade significantly as the dimensionality of the input space increases [28, 78]. This motivates the adoption of low-dimensional latent spaces through generative models. In particular, text-to-speech (TTS) models, which convert text to speech while maintaining speaker-specific characteristics, have been extensively studied and widely adopted in practice [7, 8, 55]. For this reason, a seemingly natural direction is to leverage the latent space of such models as a search space.

**Missing Component: Inverse Model.** However, dimensionality reduction strategy alone is insufficient: the latent space must also be aligned with the speaker embedding space induced by the recognition model. Without such alignment, score-guided updates lead to poorly conditioned optimization landscapes and slow convergence, even compared to a direct optimization over the raw audio space. This observation highlights the need for a generative model whose latent space is well-aligned with the template space to facilitate solving the optimization problem.

From this perspective, we identify the inverse model as a key missing component in score-based speaker impersonation. By explicitly mapping speaker embeddings back to the signal domain, an inverse model induces a search space that is both low-dimensional and structurally aligned with the impersonation objective, thereby enabling more predictable and query-efficient optimization. Constructing such an inverse model, however, is non-trivial, as speech signals exhibit substantial variability across content, prosody, and acoustic conditions, and we observe that existing TTS models only provide a loose alignment between their latent spaces and speaker-discriminative representations (See Section 4.3 for details).

## 1.2 Our Contributions

In this work, we study score-based speaker impersonation attacks under a realistic black-box setting without access to victim voice samples. By identifying inversion as the primary bottleneck in existing approaches, we design an attack framework that enables efficient exploitation of score feedback in SRSs.

Our main contributions are summarized as follows:

- **Optimization-based formulation of score-based speaker impersonation.** We formalize score-based speaker impersonation as a black-box optimization problem and analyze why direct optimization in the raw audio space is inherently inefficient.
- **Identification of inversion as the central bottleneck.** We provide a systematic analysis showing that the absence of effective feature-to-speech inversion is the key factor limiting prior score-based attacks in speaker recognition.
- **Feature-aligned inverse model for speaker embeddings.** We design a feature-to-speech inverse network with identity- and structure-constraint objectives, explicitly aligning the inverse mapping with speaker-discriminative embedding geometry.
- **Query-efficient and inversion-essential impersonation attacks.** The proposed inverse model improves query efficiency by 10× on average (up to 24×) over existing score-based attacks, and

**Table 1: Comparison of speaker impersonation attacks against SRSs. The reported number of queries corresponds to the cost of performing the attack task as defined in each original work. Ours-NES and Ours-SP denote two optimization strategies used in our attack: Natural Evolution Strategies (NES) and Subspace Projection (SP), respectively. Details of these optimization methods are described in Section 6.1.**

† : We consider FakeBob applied to speaker verification here.

Method	Victim Voice Required	Query Output	#Queries
[37]	Yes	–	0
[84]		–	0
[58]		–	0
SV2TTS [30]		–	0
Voxstructor [46]		Feature vector	$\geq 100\text{K}$
AdvTTS [87]		–	0
QFA2SR [10]		–	0
SirenAttack [20]		Score	$\geq 7.5\text{K}$
Occam [85]		Decision	$\geq 10\text{K}$
FakeBob† [9]		No	Score
<b>Ours-NES</b>	<b>No</b>	<b>Score</b>	$\approx 500$
<b>Ours-SP</b>			<b>50</b>

enables subspace projection–based impersonation [36], achieving up to 91.65% attack success rate within only 50 score queries.

- **Language-agnostic and potential defenses.** Our attacks are designed in a speaker-discriminative feature space rather than the acoustic–linguistic domain, yielding empirically validated cross-lingual generalization; we also outline potential defense directions against inversion-enabled impersonation attacks.

Anonymized source code is available at: <https://anonymous.4open.science/r/Scores-Know-Bobs-Voice-5B14>.

## 2 Related Work

We overview various threats and attack scenarios against SRSs from the perspective of speaker impersonation attacks, highlighting their scope and limitations under a score-based black-box threat model. Table 1 summarizes representative prior works from this viewpoint.

**Impersonation Attacks via Victim Information.** Several prior studies consider impersonation attacks under the assumption that the adversary has access to the victim’s voice samples or related information. This category includes human voice mimicry [37], replay attacks using recorded speech [84], and voice morphing techniques that combine acoustic characteristics from multiple speakers [58]. Although these works demonstrate the feasibility of impersonation under strong adversarial assumptions, they are inapplicable to our threat model, where such information is unavailable.

**Generative and Transfer-based Impersonation Attacks.** Several studies explore impersonation through generative models that synthesize speech mimicking a target identity. Early approaches such as SV2TTS [30] operate in white-box settings and utilize internal model information. Voxstructor [46] extends this direction to black-box models by recovering victim representations through extensive interaction with the target system, followed by training a

separate synthesis model. However, this approach requires access to feature-level outputs, which are typically treated as sensitive biometric data in deployed systems. Transfer-based approaches, including AdvTTS [87] and QFA2SR [10], further study impersonation by exploiting transferability across models, but they often require victim information during preparation.

**Adversarial Attacks.** Another line of work studies adversarial attacks against SRSs, where the attacker generates an audio signal that is accepted as a target identity while remaining close to a given source utterance. This source-audio constraint plays a central role in shaping the attack objective and has been widely studied in adversarial audio generation (e.g., [9, 10, 20]). While such attacks intersect with impersonation at the decision level, they impose an additional constraint that ties the attack to an existing source signal. As a result, adversarial attacks and score-based impersonation attacks address related but structurally distinct attack objectives.

**Query-based Black-box Impersonation Attacks.** Several works investigate impersonation attacks through black-box interaction with the target SRS, demonstrating that graded feedback—such as similarity scores or decision outcomes—can be exploited to guide an attack. These studies collectively highlight the risks associated with exposing informative verification responses. Among them, FakeBob [9] is most closely aligned with our setting, as it shows that impersonation is possible using score feedback without access to the victim’s voice. Notably, FakeBob operates over verification queries evaluated against a fixed enrolled identity, which distinguishes it from attacks that rely on source-conditioned or pairwise querying. While FakeBob was originally proposed as an adversarial attack that enforces source-audio similarity, its query cost in Tab 1 reflects this additional constraint; accordingly, we consider unconstrained score-based variants for fair comparison in our impersonation setting.

**Positioning of Our Work.** In summary, prior work on speaker impersonation spans diverse threat models, ranging from settings with access to victim-side information to those imposing source-audio constraints or requiring extensive interaction with the target system. Our work operates under the same score-based black-box threat model as prior query-based impersonation attacks (e.g., FakeBob), where the adversary has no access to the victim’s voice, and focuses on improving efficiency via inversion-aligned optimization.

## 3 Problem Setting and Threat Model

**Notations.** Distances between speaker representations are measured in a feature space  $\mathcal{X}$  via a non-negative distance function  $d_{\mathcal{X}}(\cdot, \cdot)$ . We refer to  $(\mathcal{X}, d_{\mathcal{X}})$  as the corresponding feature space equipped with a distance. We use  $\mathbb{R}^d$  to denote the  $d$ -dimensional real vector space and  $\mathbb{S}^{d-1} \subset \mathbb{R}^d$  to denote the unit hypersphere. The standard inner product between two vectors is denoted by  $\langle \cdot, \cdot \rangle$ .

### 3.1 Speaker Recognition Systems (SRSs)

SRSs process speech signals  $\mathbf{v} \in \mathcal{V}$  to make decisions based on speaker-related characteristics. They rely on a feature extractor  $F : \mathcal{V} \rightarrow \mathbb{R}^d$ , which maps an input utterance to a speaker feature vector that captures speaker-discriminative information. In modern deep learning-based SRSs, the extractor is typically implemented using neural networks such as x-vector [67] and ECAPA-TDNN [19].

Commonly, feature vectors are normalized to lie on the unit hypersphere  $\mathbb{S}^{d-1} \subset \mathbb{R}^d$ , and similarity is measured via cosine similarity. Verification decisions are made by thresholding the measured distance at  $\tau$ , which is typically selected via standard criteria<sup>1</sup> such as Equal Error Rate (EER) or minimum Detection Cost Function (MinDCF), yielding thresholds denoted by  $\tau_E$  and  $\tau_M$ , respectively.

Speaker recognition systems are typically deployed in two modes: *verification* (1:1) and *identification* (1:N). In this work, we focus exclusively on verification. Using the extractor  $F$ , the system can be described by the following two procedures:

- Enroll takes an enrollment utterance  $\mathbf{v} \in \mathcal{V}$  and returns a corresponding speaker feature vector  $t := F(\mathbf{v})$ , which is subsequently stored in the system database.
- Ver takes a test utterance  $\mathbf{v}' \in \mathcal{V}$  and the stored feature vector  $t$ , and outputs  $\mathbb{1}(d_{\mathcal{X}}(F(\mathbf{v}'), t) < \tau)$ .

### 3.2 Threat Model

We consider a score-based impersonation attack against a speaker verification system. The system is accessed through a verification interface, where a client submits a speech signal with a claimed enrolled identity and receives a verification response.

In many modern authentication deployments, verification responses are not restricted to a pure binary accept/reject decision. For cloud-based service architectures, producing fine-grained similarity scores is often a functional requirement for flexible policy enforcement (e.g., risk-based authentication), as evidenced by major providers such as Microsoft Azure and AWS [4, 48]. Even if the user interface displays only a binary decision, backend services frequently transmit verbose JSON responses containing these scores. This practice, classified as *Excessive Data Exposure* (API3:2019) by OWASP [56], allows an adversary to extract precise confidence indicators from the network traffic.

In addition, when verification is executed on a client-controlled device (on-device), we assume the adversary has full control over the execution environment. In this scenario, standard dynamic analysis techniques, such as Dynamic Binary Instrumentation (DBI), function hooking, or memory inspection, allow the adversary to intercept verification routines and inspect intermediate comparison results prior to thresholding, a capability formally recognized in mobile security testing standards [57].

Accordingly, we model the target system as a black-box oracle that provides feedback with respect to the similarity between the submitted speech and the enrolled feature vector. The adversary is characterized as follows:

- **Attacker’s goal.** The adversary aims to impersonate a fixed enrolled identity by generating a speech signal  $\mathbf{v}^* \in \mathcal{V}$  that is accepted by the verification system. Formally, the goal is to find  $\mathbf{v}^*$  such that  $d_{\mathcal{X}}(F(\mathbf{v}^*), t_v) < \tau$ , where  $t_v = F(\mathbf{v}_{\text{victim}})$  denotes the victim’s enrolled feature vector and  $\tau$  is the predefined threshold.
- **Attacker’s knowledge.** The adversary has no access to the victim’s audio  $\mathbf{v}_{\text{victim}}$ , the enrolled representation  $t$ , the training data, or the internal architecture and parameters of the feature extractor  $F$ , except for its similarity metric  $\langle \cdot, \cdot \rangle$ .

- **Attacker’s capabilities.** The adversary can submit arbitrary speech signals  $\mathbf{v} \in \mathcal{V}$  for the fixed enrolled identity and obtain a response that reveals a score  $d_{\mathcal{X}}(F(\mathbf{v}), t_v)$ .

**Score-based Impersonation Attack.** Under the system and threat models described above, a *score-based impersonation attack* considers an adversary who interacts with a speaker verification system through its verification interface and leverages score-level feedback to generate a speech signal impersonating the victim’s identity. Formally, the adversary submits speech signals  $\mathbf{v} \in \mathcal{V}$  and observes score feedback  $\langle F(\mathbf{v}), t_v \rangle$ , where  $t_v$  is victim’s enrolled feature vector. The attack succeeds if the adversary produces an utterance  $\mathbf{v}^* \in \mathcal{V}$  such that  $d_{\mathcal{X}}(F(\mathbf{v}^*), t) < \tau$  for a predefined threshold  $\tau$ .

## 4 Why Inverse Models?

In this section, we show how the inverse model serves as a core building block for score-based impersonation attacks. We model the score-based attack as a black-box optimization problem, showing the benefit of leveraging inverse models in terms of (mis)alignment between the search space and the objective. We further experimentally validate this effect, demonstrating that the proposed inverse model substantially reduces the number of optimization steps compared to baseline approaches. For clarity, we refer to our method as ‘Ours’ when presenting comparisons and figures, although full methodological details are introduced in the following section.

### 4.1 Score-based Attack as an Optimization

A typical approach to instantiate score-based impersonation attacks is to view it as the following optimization problem.

$$\text{minimize } d_{\mathcal{X}}(F(\mathbf{v}), F(\mathbf{v}^*)) \text{ s.t. } \mathbf{v}^* \in \mathcal{V} \quad (1)$$

Here, the adversary  $\mathcal{A}$  succeeds in the attack if the found solution  $\mathbf{v}^*$  from Eq. (1) satisfies  $d_{\mathcal{X}}(F(\mathbf{v}), F(\mathbf{v}^*)) < \tau$ . From this viewpoint, we can classify the existing attack methods in terms of how to solve Eq. (1) via exploiting score queries. For example, several score-based attacks like Fakebob [9] exploit zeroth-order optimization solvers, such as gradient estimation [12], genetic algorithm [3], or hill-climbing optimization [25].

**Reducing Search Space via Latents.** In the above approach,  $\mathcal{V}$  is usually high-dimensional, e.g., 48,000 (3sec \* 16khz), which renders directly solving Eq. (1) rather cumbersome. To mitigate this, one can leverage generative models with a latent space to reduce the search space. That is, for a generative model  $G : \mathcal{Z} \rightarrow \mathcal{V}$  with a latent space  $\mathcal{Z}$  having much smaller dimensionality than  $\mathcal{V}$ , we can reformulate Eq. (1) as

$$\text{minimize } d_{\mathcal{X}}(F(\mathbf{v}), F(G(z))) \text{ s.t. } z \in \mathcal{Z} \quad (2)$$

Note that this approach incurs the trade-off between the size of the search space and the quality of the solution. In an extreme case, the adversary never succeeds in the attack from solving Eq. (2) if  $G$ ’s capacity is insufficient, i.e.,  $\min_{z \in \mathcal{Z}} d_{\mathcal{X}}(F(\mathbf{v}), F(G(z))) \geq \tau$ .

### 4.2 Inverse Models for Aligning Search Space

The effectiveness of latent-space optimization in Eq. (2) depends critically on how well the latent space  $G$  is aligned with the speaker embedding space induced by  $F$ . However, for generic generative

<sup>1</sup>Detailed description of criteria is in Appendix D.1

models, proximity in the latent space does not necessarily correspond to proximity in the embedding space, leading to poorly conditioned optimization landscapes. To overcome this limitation, we introduce the inverse model as an explicit aligner between the latent space and the embedding space, enabling more predictable and efficient optimization.

**Inverse Models and Desired Properties.** Given a feature extractor  $F$ , an *inverse model*  $F^{-1} : \mathbb{S}^{d-1} \rightarrow \mathcal{V}$  of  $F$  aims to reconstruct a plausible voice  $\mathbf{v}$  that closely matches a given feature template  $t$ , i.e.,  $F^{-1}(t) = \mathbf{v}$ ,  $F(\mathbf{v}) \approx t$ . The existence of such inverse models has been reported in various biometric modalities, including face [21, 47], fingerprint [79], finger vein [34], iris [1], and palmprint [83].

From the perspective of a generative model, the latent representation of the inverse model is explicitly aligned with the feature space. Consequently, updates in the latent space induce predictable changes in the objective function  $d_{\chi}(F(\mathbf{v}), F(G(z)))$  when  $G = F^{-1}$ , making Eq. (2) substantially easier to optimize. These considerations naturally lead us to analyze the essential requirements of an inverse model for score-based impersonation attacks:

- **ID-Constraints (A1).** The output audio from the inverse model must maintain identity constraints of  $F$ , i.e.,  $\forall x \in \mathbb{S}^{d-1}, d_{\chi}((F \circ F^{-1})(x), x) < \tau$ .
- **Transferability (A2).** The generated inverse audio should be recognized as the same identity by alternative speaker recognition models.

The former (A1) implies the alignment between the feature space of a known SRS  $F$  and the latent space of its inverse. On the other hand, the latter (A2) ensures that the alignment between the latent space and other SRS models’ feature embeddings is still largely maintained. Specifically, this property is necessary when launching the score-based attack in the black-box setting; in this case, the adversary cannot access the target SRS and thus exploits the surrogate model and its inverse model. Here, thanks to (A2), such an inverse model is still effective for conducting the score-based attack based on Eq. (2) against target SRS.

**A Candidate Inverse Model: TTS.** Text-to-speech (TTS) systems generate speech signals from text while allowing certain characteristics of the output to be controlled through auxiliary inputs. Depending on the design objective of the TTS system, these auxiliary inputs may encode different factors, such as speaker identity, speaking style, or prosodic attributes.

In particular, zero-shot text-to-speech (ZS-TTS) models [53] synthesize speech for previously unseen speakers by conditioning the generation process on a speaker feature vector extracted from a short reference utterance. Although ZS-TTS models are developed for general-purpose speech synthesis and voice cloning rather than impersonation attacks, this conditioning mechanism allows them to be functionally interpreted as candidate inverse models that map speaker recognition features back to speech signals. In this work, we focus on TTS models that accept a *speaker feature vector* as an explicit conditioning input.

Based on this criterion, we consider several representative ZS-TTS models as candidate inverse models, including SV2TTS [30], Voxstructor [46], and YourTTS [8]. These models differ in architectural details but share the common mechanism of conditioning

speech generation on speaker feature vectors. Additional selection criteria and details are provided in Appendix B.

### 4.3 Challenge: Finding Good Inverse Models

The optimization-based viewpoint provides a principled pipeline for score-based impersonation attack, and the inverse model plays a crucial role. However, we observe that existing models fail to effectively realize the attack pipeline, revealing a mismatch between current training approaches and the attack objective. This motivates the design of a new inverse model specifically designed for impersonation attacks. In this section, we analyze these limitations and summarize the key takeaways. Unless otherwise specified, detailed experimental settings are deferred to Appendix C.

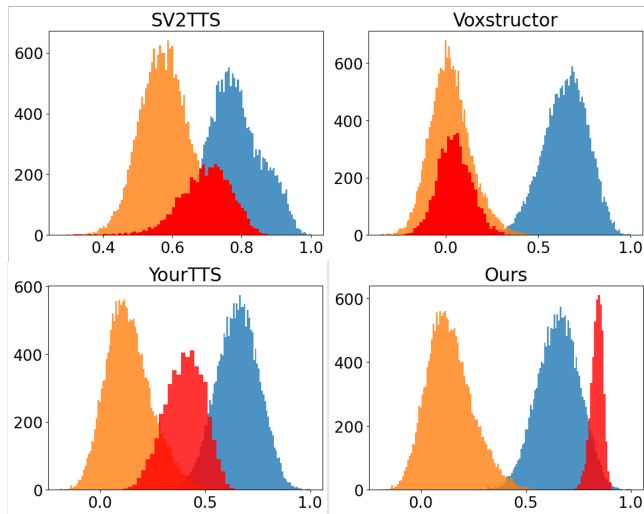
**Do Existing Candidates Satisfy the Desired Properties?** We evaluate whether existing inverse model candidates satisfy the desired identity-preserving properties under a unified round-trip evaluation protocol. Specifically, we assess (A1) identity preservation under the local speaker recognition model and (A2) transferability of the preserved identity to an alternative target model.

We consider a local speaker recognition model  $F_L$ , for which an inverse model  $F_L^{-1}$  is instantiated. Given an input utterance  $\mathbf{v}$ , we extract its speaker embedding  $x = F_L(\mathbf{v})$  and synthesize inverse audio  $\tilde{\mathbf{v}} = F_L^{-1}(x)$ . Identity preservation is evaluated by measuring the cosine similarity between speaker embeddings extracted from the original and reconstructed utterances. When evaluated using the local model  $F_L$ , the resulting similarity score is defined as  $s_L(\mathbf{v}) = \langle F_L(\mathbf{v}), F_L(\tilde{\mathbf{v}}) \rangle$ , which directly corresponds to property A1. To evaluate transferability (A2), we compute the same similarity using an alternative target speaker recognition model  $F_T$ :  $s_T(\mathbf{v}) = \langle F_T(\mathbf{v}), F_T(\tilde{\mathbf{v}}) \rangle$ . In our experiments, this protocol is applied to utterances from the VoxCeleb1 test set. For reference, we compare the resulting round-trip similarity distributions against positive (same-speaker) and negative (different-speaker) score distributions under each evaluation model.

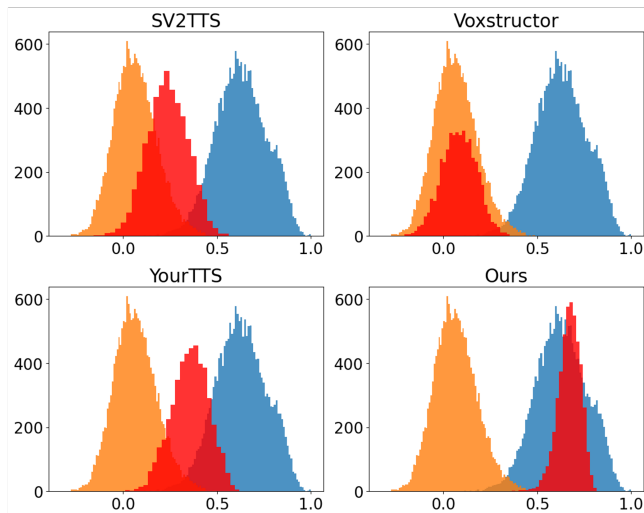
Figure 1 shows the round-trip similarity distributions evaluated by the local model  $F_L$ , corresponding to property (A1). For existing TTS-based inverse model candidates, the distributions of  $s_L(\mathbf{v})$  are clearly shifted toward those of negative pairs. That is, the reconstructed utterances  $\tilde{\mathbf{v}}$  fail to preserve speaker identity even when evaluated by the same model that produced the original embeddings, revealing weak identity preservation in the round-trip mapping.

Figure 2 further evaluates the same inverse samples under an alternative target model  $F_T = T_1$ , corresponding to property (A2). (More results on various target models is given in Appendix C.2) Compared to the local evaluation, the separation between the round-trip similarity distribution and the positive reference further degrades, and the distributions overlap more closely with negative pairs. This observation suggests that any residual identity information retained under  $F_L$  does not reliably transfer across speaker recognition models, indicating poor cross-model generalization.

Taken together, these results demonstrate that existing inverse model candidates fail to jointly satisfy the desired properties defined in Section 4.2. In particular, they exhibit neither strong identity preservation under the local model (A1) nor robust transferability to unseen target models (A2).



**Figure 1: Distributions of round-trip similarity scores  $s_L(\mathbf{v})$  (red) evaluated on the local speaker recognition model  $F_L$ . Positive (blue) and negative (orange) reference distributions are shown for comparison. Best viewed in color.**



**Figure 2: Distributions of round-trip similarity scores  $s_T(\mathbf{v})$  (red) evaluated on the  $F_T = T_1$ . Positive (blue) and negative (orange) reference distributions are shown for comparison. Best viewed in color.**

**Trade-Off from Latent Space Reduction.** Recall that the latent space reduction strategy incurs the trade-off between the query complexity and the accuracy of the solution. To capture this, we introduce the following two metrics to quantify each component of the trade-off in terms of score-based impersonation attack for a fixed optimization solver, e.g., gradient estimation by NES.

- (Metric Projection) How close the solution of Eq. (2) is to the target voice, i.e.,  $d_{\mathcal{X}}(\mathbf{v}; G) := \min_{z \in \mathcal{Z}} d_{\mathcal{X}}(F(\mathbf{v}), F(G(z)))$ .
- (Optimization Trajectory) How many optimization steps are required to succeed in the attack, i.e., the smallest  $t$  such that  $d_{\mathcal{X}}(F(\mathbf{v}), F(G(z_t))) < \tau$  after  $t$  score queries.

The former examines whether the adversary can succeed in the attack with an unlimited query budget, whereas the latter measures the (expected) query complexity.

Figure 3 compares the optimization trajectories of different inverse model candidates under using two different batch sizes (num. queries for calculating optimization gradients),  $B = 50$  and  $B = 10$ , evaluated against the target model ( $L$ : feature extractor of YourTTS) in a black-box setting. The x-axis denotes the cumulative number of score queries, and the y-axis reports the projection metric  $d_{\mathcal{X}}(F(\mathbf{v}), F(\mathbf{v}_t^*))$ .

Audio-space optimization shows similar behavior across both budgets, requiring a large number of total queries to make noticeable progress. This reflects the high per-step query cost incurred by gradient estimation in the audio space, which limits the number of effective update steps. Latent-space optimization substantially reduces this cost, but its effectiveness depends critically on how well the latent space aligns with the feature space.

This difference is evident when comparing YourTTS with our inverse model. Although both methods operate in a low-dimensional latent space, YourTTS exhibits early saturation and slow improvement after an initial decrease in the projection metric. This suggests that, while gradient estimation is feasible, the resulting gradients are weakly aligned with the impersonation objective. In contrast, our inverse model maintains a consistently steep trajectory, indicating that its latent representation provides more informative gradients for speaker similarity optimization.

As a result, the gap between our method and YourTTS widens in the low-query regime. While YourTTS benefits from dimensionality reduction, it fails to fully translate additional optimization steps into improved projection accuracy. These results indicate that reducing dimensionality is necessary but not sufficient: the latent space must also be structured to reflect the geometry of the target feature space.

In the next sections, we present our method for building the inverse model and completing the impersonation attack.

## 5 The Proposed Inverse Model

Our approach constructs an inverse model by fine-tuning a pre-trained TTS model. The training procedure consists of three key components: (1) a fixed-text strategy, (2) specialized loss functions, and (3) strategic parameter freezing.

### 5.1 Framework: Fixed-Text Fine-Tuning

Our core idea is to adapt a pre-trained TTS model to approximate the inverse of a given speaker recognition model  $F$ . A fundamental obstacle is that speaker recognition datasets lack aligned text labels, rendering conventional TTS fine-tuning inapplicable. To overcome this issue, we employ a *fixed-text strategy*, which fixes a pre-defined text sequence as the TTS input during fine-tuning.

This strategy offers two key advantages. First, it enables the use of large-scale, text-unlabeled speaker recognition datasets for training, allowing the inverse model to be optimized directly on the data distribution learned by the target model it aims to invert. Second, by decoupling constant linguistic content from variable speaker identity, the model is forced to allocate its learning capacity exclusively to mapping a given speaker embedding to its corresponding vocal

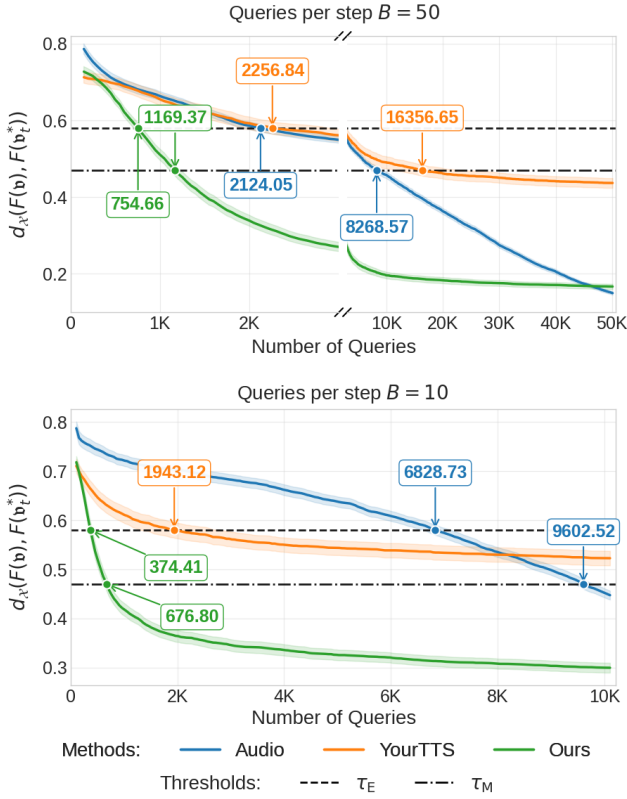


**Figure 3: Optimization trajectories of score-based impersonation attacks on various search spaces. Curves show the mean of the best cosine distance with 95% CI. Best viewed in color.**

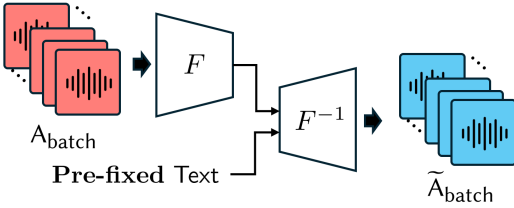


**Figure 4: Fixed-text Strategy for Fine Tuning Inverse Model.**

characteristics. Fixing the linguistic content implicitly regularizes training by eliminating variability unrelated to speaker identity.

### 5.2 Loss Function Design for the Inverse Model

To train the inverse model effectively, we introduce two complementary loss functions: an *ID-constraints loss* for enforcing sample-level fidelity and a *structure-constraints loss* for preserving the geometry of the speaker embedding space.

**ID-Constraints Loss ( $L_{IC}$ ).** At the sample level, this loss enforces a one-to-one identity correspondence between an original audio sample  $aud_i$  and its synthesized counterpart  $\widetilde{aud}_i$  by maximizing the similarity of their speaker embeddings. This loss directly promotes

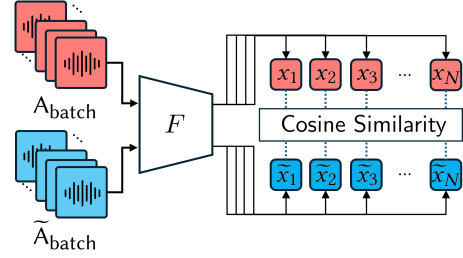


**Figure 5: ID-Constraints Loss  $L_{IC}$ .** Given an audio batch  $A_{batch}$ , the cosine similarities for each sample pair are computed using the set of synthesized samples  $\widetilde{A}_{batch}$  generated through the process illustrated in Figure 4.

property **A1**.

$$L_{IC} = \frac{1}{N} \sum_{i=1}^N (1 - \langle F(aud_i), F(\widetilde{aud}_i) \rangle),$$

where  $\widetilde{aud}_i = F^{-1}(F(aud_i), \text{Text})$ ,  $N$ =size of batch.

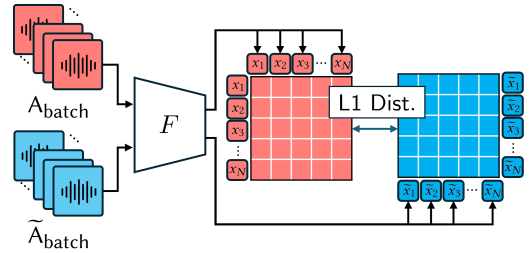


**Figure 6: ID-Constraints Loss  $L_{IC}$ .** Given an audio batch  $A_{batch}$ , the cosine similarities for each sample pair are computed using the set of synthesized samples  $\widetilde{A}_{batch}$  generated through the process illustrated in Figure 4.

**Structure-Constraints Loss ( $L_{SC}$ ).** At the batch level, this loss preserves the relational structure of the speaker embedding space. Specifically, it enforces consistency between the pairwise similarity matrix of original samples,  $S$ , and that of synthesized samples,  $\widetilde{S}$ . By preserving relative distances between speaker embeddings, this loss encourages the inverse model to respect the global geometry of the speaker space, which is critical for generalization and transferability (property **A2**).

$$L_{SC} = \frac{1}{N^2} \sum_{i=1}^N \sum_{j=1}^N |S_{i,j} - \widetilde{S}_{i,j}|,$$

where  $S_{i,j} = \langle F(aud_i), F(aud_j) \rangle$  and  $\widetilde{S}_{i,j} = \langle F(\widetilde{aud}_i), F(\widetilde{aud}_j) \rangle$ .

**Final Loss.** The final training objective is a weighted combination of the two losses:

$$L_{Total} = \lambda_{IC} L_{IC} + \lambda_{SC} L_{SC}.$$

Together, these losses ensure that the inverse model learns a structured and transferable mapping aligned with the speaker embedding space, rather than merely memorizing individual identities.

### 5.3 Setting of Trainable Parameters

Given the fixed-text strategy, we freeze all text-related components of the TTS model, including the text encoder and the duration predictor. Since the linguistic content remains constant, their pre-trained representations are sufficient. Training updates are therefore concentrated on the speaker encoding and audio synthesis components, focusing the model capacity on learning the mapping from a speaker embedding  $F(\text{aud}_i)$  to the corresponding synthesized audio  $\widehat{\text{aud}}_i$ . This design yields a compact and stable optimization space, which is essential for query-efficient gradient estimation in subsequent black-box attacks. Further details are provided in Appendix D.2.3.

## 6 Experiments

In this section, we evaluate the proposed inverse model under score-based black-box speaker impersonation attacks. We first introduce two attack instantiations that leverage the inverse model in complementary ways: one based on iterative score-based optimization, and the other based on a single-step inference exploitation of score-level structural information. This is followed by a description of the experimental setup and evaluation protocol.

We present quantitative results for the two attack settings and, to better understand the factors underlying these results, we further analyze the impact of the inverse-model training objectives through controlled ablation experiments. Finally, we examine how the proposed framework can be generalized across languages.

### 6.1 Attack Instantiation Using the Proposed Inverse Model

We evaluate the proposed inverse model under two score-based black-box speaker impersonation attacks, denoted as **Ours-NES** and **Ours-SP**. In both settings, the attacker can only query a target speaker recognition system  $T$  for similarity scores and has no access to its internal parameters. The attacker additionally possesses a speaker recognition model  $F$  and its inverse  $F^{-1}$ , constructed independently of  $T$ . The two attacks differ in how the inverse model is utilized during the attack.

**Ours-NES.** Ours-NES performs adaptive score-based optimization in the latent space induced by the inverse model. At each iteration, a latent variable  $z \in \mathcal{Z}$  is updated using Natural Evolution Strategies (NES) [78] based on score queries to  $T$ , and decoded into an audio sample via  $b_t = F^{-1}(z_t)$ .

Although Ours-NES operates under the same black-box threat model as FakeBob, the two attacks are fundamentally different in formulation. FakeBob is proposed as an adversarial perturbation attack and enforces explicit noise-norm constraints around a source audio. In contrast, Ours-NES directly optimizes for speaker impersonation without relying on a source audio or imposing any audio-domain perturbation constraints, treating the inverse model as a generative prior for producing valid attack samples.

**Ours-SP.** Ours-SP instantiates a non-adaptive impersonation attack [36] that exploits the structural similarity between the target system and a locally available speaker recognition model. Rather than performing iterative optimization, Ours-SP leverages the fact

that similarity scores produced by models trained for the same task often preserve consistent geometric structure.

Concretely, the attacker queries the target system  $T$  with a set of audio samples  $\{\mathbf{v}_i\}$  and observes the corresponding scores  $s_i = T(\mathbf{v}_i)$ . Assuming structural alignment between the target system and the local model  $F$ , these scores can be approximated as  $s_i \approx \langle F(\mathbf{v}_i), F(e) \rangle$ , where  $e$  denotes the enrolled voice. This relation allows the attacker to derive, in a purely mathematical manner, an estimate  $\hat{x}$  of the victim’s speaker embedding under the local model by solving a linear system. To ensure numerical stability, the query set is constructed to be approximately orthogonal in the embedding space, formalized as a  $\delta$ -orthogonal biometric set.

Crucially, recovering such a speaker embedding alone is insufficient to mount a practical impersonation attack. Without a feasible inverse model, there is no direct way to convert the reconstructed embedding  $\hat{x}$  into a valid audio sample. The proposed inverse model fills this gap by mapping  $\hat{x}$  back to the audio domain, yielding an impersonating audio sample  $b^* = F^{-1}(\hat{x})$ . In this sense, the inverse model serves as an essential tool that transforms score-level structural leakage into an executable speaker impersonation attack. (More details in Appendix E)

**Summary.** Ours-NES and Ours-SP represent two complementary ways of exploiting the same inverse model for score-based black-box impersonation. Ours-NES emphasizes adaptive optimization in a compact latent space, whereas Ours-SP relies on mathematically deriving a victim’s speaker embedding in local model space from score queries and executing the attack via inversion.

### 6.2 Experimental Setting

To construct a comprehensive experimental environment, we selected five open-source SR models ( $T_1$ – $T_5$ ) as our targets. Our selection strategy was designed to establish diverse evaluation conditions based on model architecture, and the training data’s relationship to our local model ( $L$ ). Specifically,  $T_1$  through  $T_4$  were trained on a dataset completely disjoint from  $L$ , allowing evaluation in a context with no data domain overlap. In contrast,  $T_5$  was trained on a substantially larger and more diverse collection of datasets that partially overlaps with our own, enabling evaluation against a more powerful and well-generalized target.

For each model, we set acceptance thresholds by calculating the standard Equal Error Rate (EER) and the minimum Detection Cost Function (minDCF). In Appendix D.3, we provide the specific details for each model, including their architectures, training datasets, performance, and the resulting acceptance thresholds ( $\tau_E$ ,  $\tau_M$ ).

We use the Attack Success Rate (ASR) as an evaluation metric for impersonation attacks, which is the proportion of generated attack audio samples ( $\widehat{\text{aud}}_i$ ) that the target SRS successfully verifies as belonging to the same identity as their corresponding target audio samples ( $\text{aud}_i$ ). The ASR can be formulated as follows: 
$$\text{ASR} = \frac{\sum_{i=1}^{|\mathcal{D}_{\text{test}}|} \mathbb{1}(D_{\mathcal{X}}(F_T(\text{aud}_i), F_T(\widehat{\text{aud}}_i)) < \tau_{\text{target}})}{|\mathcal{D}_{\text{test}}|}$$
 where  $\mathcal{D}_{\text{test}}$  represents the set of test audio samples,  $\text{aud}_i \in \mathcal{D}_{\text{test}}$  refers to each target audio sample,  $F_T$  is the target SRS’s feature extractor,  $\widehat{\text{aud}}_i$  is the generated attack audio corresponding to  $\text{aud}_i$ ,  $\tau_{\text{target}}$  is the target SRS’s decision threshold for verification, and  $\mathbb{1}(\cdot)$  is the indicator function (1 if true, 0 otherwise). An attack succeeds for  $\text{aud}_i$  if the

**Table 2: Specifications of target SR models ( $T_1$ – $T_5$ ) and local model ( $L$ ), including architectures, trainsets, and thresholds defined on EER, minDCF (resp.  $\tau_E$ ,  $\tau_M$ ). Detailed EER and minDCF performance metrics are in Table 13.**

Model	Architecture	Trainset	$\tau_E$	$\tau_M$
$T_1$	Redim-S [81]	VoxBlink2	0.6605	0.5518
$T_2$	Redim-M [81]	VoxBlink2	0.6624	0.5437
$T_3$	SimAMResNet34 [62]	VoxBlink2	0.6256	0.5060
$T_4$	SimAMResNet100 [62]	VoxBlink2	0.6135	0.4932
$T_5$	Titanet-L [39]	VoxCeleb1,2+ $\alpha$	0.6654	0.5215
$L$	H/ASP [27]	VoxCeleb1,2	0.5778	0.4667

similarity between  $F_T(\text{aud}_i)$  and  $F_T(\widehat{\text{aud}}_i)$  exceeds  $\tau_{\text{target}}$ . In our evaluation,  $\mathcal{D}_{\text{test}}$  is instantiated using the VoxCeleb1 test set for English and the CNCeleb test–enrollment split for Chinese. For NES-based attacks, we randomly subsample 100 target audio samples from  $\mathcal{D}_{\text{test}}$  due to the high query cost per sample, and compute ASR over this subset.

### 6.3 Evaluation of Ours-NES

**Baselines.** We compare **Ours-NES** against several score-based and generative impersonation baselines under the same black-box threat model.

*Audio-NES.* Audio-NES estimates gradients directly in the waveform space by injecting random perturbations and observing score variations from the target system. This approach is conceptually closest to prior score-based attacks such as FakeBob. However, FakeBob is originally formulated as an adversarial perturbation attack and assumes the existence of a source utterance together with an explicit noise-norm constraint.

To ensure a fair comparison under our impersonation setting, where no source audio is not essential, we modify the setup as follows. Audio-NES is initialized from a randomly sampled 3-second audio signal and performs unconstrained optimization without any perturbation budget. This configuration removes advantages stemming from source-audio proximity and isolates the effect of optimizing directly in the audio space.

*YourTTS-NES.* YourTTS-NES follows the same NES-based optimization as Ours-NES, but replaces the proposed inverse model with YourTTS.

*Excluded candidates.* We do not include SV2TTS and Voxstructor as NES-based baselines. Both methods require repeated inner-loop synthesis or reconstruction steps, making them prohibitively slow for iterative score-based optimization. Moreover, our earlier analysis shows that their speaker identity control and local speaker-discriminative alignment are substantially weaker than those of YourTTS. As a result, they are dominated both computationally and in attack effectiveness, and are therefore omitted from the NES-based comparison.

*Implementation details.* While all NES-based attacks follow the same score-based optimization paradigm, their concrete implementations differ depending on the underlying optimization space. In

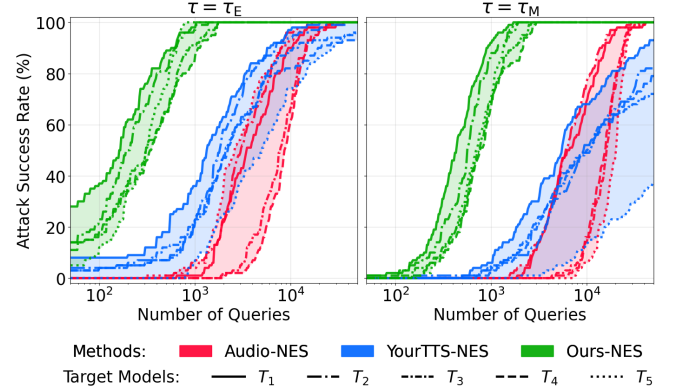


**Figure 7: Attack success rate as a function of the number of score queries for NES-based impersonation attacks. Results are shown for two decision thresholds,  $\tau_E$  (left) and  $\tau_M$  (right), across five target speaker recognition models ( $T_1$ – $T_5$ ).**

**Table 3: Comparison of ASR and query efficiency under  $\tau_{\text{target}} = \tau_E$  and  $\tau_M$ . The query budget is 50k. Each cell reports the ASR (top) and the average number of queries calculated over successful attacks (bottom).**

Method	$T_1$	$T_2$	$T_3$	$T_4$	$T_5$	Avg.
$\tau_{\text{target}} = \tau_E$						
Audio-NES	100.0% (5.2k)	100.0% (4.3k)	100.0% (8.7k)	100.0% (9.5k)	100.0% (3.8k)	100.0% (6.3k)
YourTTS-NES	100.0% (2.5k)	100.0% (3.4k)	96.0% (4.1k)	93.0% (4.2k)	96.0% (7.9k)	97.0% (4.4k)
<b>Ours-NES</b>	<b>100.0%</b> <b>(0.2k)</b>	<b>100.0%</b> <b>(0.3k)</b>	<b>100.0%</b> <b>(0.4k)</b>	<b>100.0%</b> <b>(0.5k)</b>	<b>100.0%</b> <b>(0.3k)</b>	<b>100.0%</b> <b>(0.3k)</b>
$\tau_{\text{target}} = \tau_M$						
Audio-NES	100.0% (8.5k)	100.0% (7.6k)	100.0% (16.3k)	100.0% (16.1k)	100.0% (19.3k)	100.0% (13.6k)
YourTTS-NES	93.0% (8.9k)	82.0% (11.5k)	72.0% (8.9k)	79.0% (11.3k)	37.0% (18.8k)	72.6% (11.0k)
<b>Ours-NES</b>	<b>100.0%</b> <b>(0.5k)</b>	<b>100.0%</b> <b>(0.6k)</b>	<b>100.0%</b> <b>(0.9k)</b>	<b>100.0%</b> <b>(1.0k)</b>	<b>100.0%</b> <b>(0.8k)</b>	<b>100.0%</b> <b>(0.8k)</b>

particular, the parameterization, noise injection strategy, and decoding process vary across audio-space, and inverse-latent-space optimization. We describe these differences and the corresponding algorithmic instantiations in detail in Appendix D.2. For NES-based methods, we report results from the best-performing setting among the tested values of  $B = 10, 50$  with 1K iteration steps and in case of comparable performance, we choose the case with fewer queries.

**Analysis of NES-based Impersonation Results.** Figure 7 and Table 3 jointly summarize the effectiveness and query efficiency of NES-based speaker impersonation attacks. Across all five target speaker recognition systems, **Ours-NES** consistently achieves superior performance in terms of both attack success rate (ASR) and query efficiency under the same black-box threat model.

Under the EER threshold, all methods are eventually able to achieve high ASR given a sufficiently large query budget. However, the required number of queries differs substantially across methods.

As shown in Table 3, Audio-NES requires on average 6.3k queries to succeed, reflecting the difficulty of directly optimizing in the high-dimensional waveform space. YourTTS-NES reduces this number to 4.4k queries on average by operating in a lower-dimensional generative latent space. In contrast, Ours-NES achieves 100% ASR across all target models with only 0.3k queries on average, corresponding to more than an order-of-magnitude reduction in query complexity. This trend is consistent with the success curves in Figure 7, where Ours-NES exhibits rapid and stable convergence within a few hundred queries.

The performance gap becomes more pronounced under the stricter minDCF threshold. While Audio-NES still attains 100% ASR at the cost of a substantially increased query budget (13.6k queries on average), YourTTS-NES exhibits a notable degradation in attack success, achieving only 72.6% ASR on average. This degradation is most severe for  $T_5$ , where the ASR of YourTTS-NES drops to 37.0% despite consuming up to 18.8k queries. These results indicate that, beyond a certain point, increasing the query budget alone is insufficient to overcome structural misalignment between the optimization space and the target decision boundary.

The failure cases observed for YourTTS-NES can be interpreted as worst-case manifestations of the trade-off discussed in Section 4.3. When the latent space of a generative model is insufficiently aligned with the speaker-discriminative embedding geometry of the target system, score-based optimization may converge to regions that produce natural-sounding speech but remain consistently below stringent acceptance thresholds. In such poorly aligned scenarios, impersonation attacks may become largely ineffective rather than merely less query-efficient, as exemplified by the behavior on  $T_5$  under the minDCF threshold.

In contrast, Ours-NES maintains 100% ASR across all target systems and thresholds, including these worst-case settings, with an average of only 0.8k queries under the minDCF criterion. This robustness stems from the inverse-model-induced latent space, which is explicitly trained to preserve speaker identity with respect to a speaker recognition model. By aligning the optimization space with speaker-discriminative structure, Ours-NES enables stable gradient estimation and effective score exploitation even under stringent decision boundaries.

**Takeaway.** Overall, these results highlight that the effectiveness of score-based speaker impersonation is fundamentally determined by the choice of the optimization space. Simply adopting a generic generative prior is insufficient to ensure reliable attacks across target systems. In contrast, an inverse-model-induced latent space that is explicitly aligned with speaker-discriminative feature geometry enables both query-efficient and robust black-box impersonation. This alignment allows stable score exploitation even under stringent decision thresholds, making the inverse model a key component of practical score-based impersonation attacks.

## 6.4 Evaluation of Ours-SP

**Baselines.** Ours-SP is a non-adaptive, one-step impersonation attack that reconstructs a victim’s feature vector in local space from score queries and executes the attack via inversion. Since no iterative optimization is involved, all baselines can be evaluated under the same query budget (=50, detailed in Appendix D.2.7). [78]

*SV2TTS, Voxstructor and YourTTS.* For SV2TTS, Voxstructor, and YourTTS, we generate attack utterances by conditioning the models on speaker representations estimated via subspace projection in the local feature space. The projected speaker vector is used as the conditioning input to synthesize a single utterance per attack.

*Audio-GD.* Audio-GD (Gradient Descent) operates in the same search space as Audio-NES, namely the raw audio domain, but differs fundamentally in its objective. Instead of optimizing the target system’s score directly, Audio-GD minimizes the distance between the embedding of the generated audio and a reconstructed *local* speaker embedding under the attacker’s local model. (Detailed in Appendix D.2.8) This setting isolates the effect of local embedding recovery while removing the need for an inverse mapping.

**Analysis of SP-based Impersonation Results.** Table 4 summarizes the attack success rates (ASRs) of Ours-SP and baseline methods against five target speaker recognition systems under both the EER-derived threshold  $\tau_E$  and the stricter minDCF-derived threshold  $\tau_M$ . All methods are evaluated under the same query budget and generate a single attack utterance, allowing for a direct comparison of their practical effectiveness.

Across all target systems and both threshold settings, **Ours-SP** consistently achieves substantially higher ASRs than all baseline approaches. For example, on  $T_1$ , Ours-SP attains an ASR of 91.65% at  $\tau_E$  and 59.83% at  $\tau_M$ , whereas the strongest baseline (YourTTS) reaches only 15.99% and 2.70%, respectively. Similar performance gaps are observed across  $T_2$ – $T_5$ , indicating that the proposed method generalizes well across heterogeneous target systems even without iterative score optimization.

Baseline TTS-based approaches, including SV2TTS, Voxstructor, and YourTTS, rely purely on the generative capability of pretrained models conditioned on inferred speaker representations. Since these methods do not exploit score-level structural information from the target system, their success rates remain low, particularly under the stricter threshold  $\tau_M$ . This limitation highlights that generative priors alone are insufficient to reliably produce utterances that cross target decision boundaries.

Audio-GD represents a stronger baseline that attempts to recover a speaker embedding by minimizing the distance between the generated audio and a reconstructed *local* speaker embedding. While this approach partially leverages speaker-discriminative information, it still exhibits low and unstable ASRs across most target systems. This behavior suggests that local embedding recovery alone does not guarantee effective transfer to the target system, especially when the local and target embedding spaces are misaligned. In such cases, the absence of an identity-preserving inverse mapping prevents the reconstructed representation from being translated into a successful impersonation.

An exception is observed for  $T_5$ , where Audio-GD achieves relatively higher ASRs. This behavior can be attributed to improved alignment between the local and target embedding spaces, potentially due to partial overlap in training data or architectural similarity. Even in this more favorable setting, however, Audio-GD remains substantially less effective than Ours-SP, underscoring the importance of effective inversion.

**Table 4: ASRs comparing the proposed method against alternative baseline approaches attacking  $T_1$ – $T_5$ . Target thresholds ( $\tau_{\text{target}}$ ) are derived from EER ( $\tau_E$ ) and minDCF ( $\tau_M$ ) for each target model.**

Method	$T_1$		$T_2$		$T_3$		$T_4$		$T_5$	
	$\tau_E$	$\tau_M$								
SV2TTS	1.57%	0.04%	0.87%	0.02%	0.59%	0.00%	0.42%	0.00%	0.02%	0.00%
Voxstructor	0.11%	0.00%	0.02%	0.00%	0.02%	0.00%	0.01%	0.00%	0.00%	0.00%
Audio-GD	4.65%	0.15%	6.37%	0.19%	1.38%	0.02%	0.30%	0.00%	34.36%	4.89%
YourTTS	15.99%	2.70%	11.62%	1.57%	10.58%	1.72%	7.99%	1.57%	0.28%	0.00%
<b>Ours-SP</b>	<b>91.65%</b>	<b>59.83%</b>	<b>85.47%</b>	<b>44.33%</b>	<b>76.23%</b>	<b>34.54%</b>	<b>62.23%</b>	<b>19.86%</b>	<b>68.46%</b>	<b>17.03%</b>

**Takeaway.** Overall, these results show that reconstructing speaker-discriminative representations from score queries alone is insufficient for practical impersonation. Without an effective inverse mapping, recovered embeddings often fail to translate into speech that crosses the target decision boundary. The proposed inverse model enables identity-preserving translation from reconstructed representations to speech, making one-step SP-based impersonation feasible under realistic query budgets.

## 6.5 Effect of Inverse-Model Training Objectives

Table 5 analyzes how the proposed training objectives influence the behavior of the inverse model. In the NES-based setting, incorporating the identity-constraint loss ( $L_{IC}$ ) substantially improves attack success and query efficiency. However, applying  $L_{IC}$  in isolation may still encourage overfitting to local speaker-discriminative features. This effect is most clearly manifested in the results on  $T_5$ , where the NES-based attack exhibits a severe drop in success rate despite reduced query counts. Such behavior suggests that overfitting induced by  $L_{IC}$  can distort the structural similarity required for effective score-based optimization against different target systems. By further incorporating the structure-constraint loss ( $L_{SC}$ ), the inverse model preserves the geometry of the speaker embedding space, leading to consistently high success rates across all targets and a significant reduction in the number of required queries.

A similar but more implicit trend is observed in the SP-based setting. Although SP-based attacks do not involve iterative optimization, adding  $L_{IC}$  alone already enables effective one-shot impersonation by enforcing speaker identity. Nevertheless, the additional gains achieved by incorporating  $L_{SC}$  indicate that structural regularization also improves cross-model transferability in the one-shot regime. Taken together, these results confirm that  $L_{IC}$  and  $L_{SC}$  play complementary roles:  $L_{IC}$  ensures identity fidelity, while  $L_{SC}$  mitigates overfitting and preserves structural compatibility necessary for robust and transferable impersonation.

## 6.6 Lingual Generalization: Chinese Speaker Recognition

Our framework is designed to operate in the speaker embedding space and does not rely on linguistic content. As such, its applicability is not inherently tied to any specific language. To further support this claim, we provide an additional evaluation on Chinese speaker recognition systems for providing additional empirical evidence for the language-agnostic nature of the proposed framework.

**Table 5: Ablation study on inverse-model training objectives. For NES-based, we report ASR (%) at  $\tau_M$  together with the average number of score queries over successful attacks (in parentheses). For SP-based, we report ASR (%) at  $\tau_E$ .  $L_{IC}$ : Identity-Constraint loss,  $L_{SC}$ : Structure-Constraint loss.**

Attack Method	$F^{-1}$	Target SR models				
		$T_1$	$T_2$	$T_3$	$T_4$	$T_5$
NES	YourTTS	93.0% (8.9k)	82.0% (11.5k)	72.0% (8.9k)	79.0% (11.3k)	37.0% (18.8k)
	+ $L_{IC}$	100% (1.7k)	100% (1.9k)	100% (2.5k)	99.0% (2.8k)	6.0% (1.3k)
	+ $L_{IC} + L_{SC}$	<b>100%</b> <b>(0.5k)</b>	<b>100%</b> <b>(0.6k)</b>	<b>100%</b> <b>(0.9k)</b>	<b>100%</b> <b>(1.0k)</b>	<b>100%</b> <b>(0.8k)</b>
SP	YourTTS	15.99%	11.62%	10.58%	7.99%	0.34%
	+ $L_{IC}$	71.37%	56.29%	45.58%	29.21%	64.80%
	+ $L_{IC} + L_{SC}$	<b>91.65%</b>	<b>85.47%</b>	<b>76.23%</b>	<b>62.23%</b>	<b>68.46%</b>

**Table 6: Specifications of CN target SR models ( $C_1$ – $C_2$ ) and local model ( $L_{CN}$ ), including architectures, trainsets, and thresholds defined on EER, minDCF (resp.  $\tau_E$ ,  $\tau_M$ ).**

Model	Architecture	Trainset	$\tau_E$	$\tau_M$
$C_1$	CAM++ [74]	N/A	0.7064	0.4817
$C_2$	ERes2Net [14]	N/A	0.6350	0.4617
$L_{CN}$	ResNet34 [16]	CN-Celeb 1,2	0.7349	0.5043

Specifically, we train an inverse model  $L_{CN}^{-1}$  of Chinese local speaker recognition model  $L_{CN}$  using CN-Celeb1,2. We then evaluate the proposed attacks against two Chinese target systems ( $C_1$ ,  $C_2$ ) under the same black-box threat model, where the attacker can only observe similarity scores from the target system.

**Evaluation Settings.** We consider two Chinese target speaker recognition systems ( $C_1$ ,  $C_2$ ) and one Chinese local model ( $L_{CN}$ ). The target systems are adopted from the *3D-Speaker* [13] toolkit and are trained on large-scale Chinese speech corpora. While the exact training datasets are not publicly disclosed, the model descriptions report training on the order of 200k speaker identities. Although the exact training datasets are not publicly disclosed, these models are developed independently from our local training setup.

**Table 7: Attack success rates (ASR, %) on Chinese speaker recognition systems. For Ours-NES, the average number of score queries computed over successful attacks is reported in parentheses. Target thresholds are derived from EER ( $\tau_E$ ) and minDCF ( $\tau_M$ ).**

Method	$C_1$		$C_2$	
	$\tau_E$	$\tau_M$	$\tau_E$	$\tau_M$
Ours-NES	100% (0.2k)	100% (1.4k)	100% (0.2k)	100% (0.6k)
Ours-SP	71.43%	4.08%	87.76%	16.84%

The detailed architectures, training data descriptions, verification performance, as well as experimental settings and implementation details for the Chinese experiments are provided in Appendix D.2.

**Evaluation Results.** Table 7 summarizes the attack results on the Chinese target systems. Despite the language shift, Ours-NES achieves a 100% ASR across both target systems under both EER- and minDCF-derived thresholds. Moreover, successful attacks require only a small number of score queries on average, remaining within the same order of magnitude as observed in the English setting. This indicates that the inverse-model-induced latent space remains well aligned with speaker-discriminative geometry even when trained on non-English voice data.

Ours-SP also remains effective in the Chinese setting, achieving high ASRs under the EER-based threshold and non-trivial success rates under the stricter minDCF-based threshold. While performance naturally degrades as the decision threshold becomes more stringent, the attack remains practically viable. Taken together, these results show that the effectiveness and query efficiency of inverse-model-based score exploitation are preserved across languages, reinforcing the generality of the proposed framework.

## 7 Discussion

We discuss representative defenses, an exploratory cross-lingual setting, and practical limitations regarding commercial API evaluation to contextualize our results. These analyses clarify the scope of our threat model and highlight directions for future work.

### 7.1 Defense Methods

**Deepfake Detection.** Since our attack produces synthetic speech via an inverse model rather than replaying genuine recordings, we briefly explored whether a deepfake detector [26] would flag such samples. This experiment is intended as a lightweight, prototype-level probe rather than a systematic evaluation; detailed settings and results are provided in Appendix F.1.

Under this single tested configuration, we observed that audio generated by our inverse model was less frequently classified as spoofed than audio synthesized by the baseline YourTTS. This observation should not be interpreted as a general limitation of deepfake detection, which remains one of the strongest candidate defenses against synthetic speech. Rather, the result may reflect a distribution mismatch between the detector’s training data and the characteristics of audio produced by our inverse model.

In particular, our inverse model is optimized to satisfy feature-level identity constraints, which differs from the objectives of standard speech generation models. As a result, the resulting audio may exhibit artifacts that are atypical from the perspective of existing detectors. From a defensive viewpoint, such samples could potentially be used as out-of-distribution or hard examples to improve detector robustness. We leave a systematic investigation of this possibility to future work.

**Liveness Detection.** Another important line of defense is liveness detection, which aims to distinguish live human speech from replayed or synthesized inputs [2], often via interactive or auxiliary signals beyond static audio. We emphasize that our threat model does not incorporate such mechanisms: the proposed attack targets score-based speaker verification in non-interactive settings and does not attempt to bypass liveness-based defenses. Accordingly, our should not be interpreted as evidence of effectiveness against liveness detection. Nevertheless, liveness detection remains a strong and practically relevant defense, and understanding its interaction with feature-level attacks is an important direction for future work.

### 7.2 Cross-Lingual Attack Evaluation

We include a brief exploratory analysis to highlight an interesting cross-lingual scenario. In this setting, the local speaker recognition model, the inverse model, and the attack inputs are all based on English data, while only the target speaker verification system is trained on a different language (Chinese). From the target system’s perspective, the resulting attack queries therefore constitute out-of-distribution inputs from the perspective of language. (Detailed in Appendix F.2)

Despite this mismatch, we observe that impersonation attacks can still succeed under certain operating points. Importantly, this observation reflects the cross-lingual properties of speaker representations learned by the target SRS, which our attack exploits, and should not be confused with the language-agnostic design of our overall framework, demonstrated in Section 6.6. We emphasize that this experiment is intended to spark interest rather than provide a comprehensive evaluation, and we leave a systematic study of cross-lingual robustness to future work.

### 7.3 Limitation on Commercial API Evaluation

We acknowledge the importance of evaluating speaker impersonation attacks against commercial SRS APIs, which are widely deployed in practice. However, by early 2025, major providers had enforced strict Responsible AI policies that restrict or prohibit academic testing of hosted speaker verification endpoints. To comply with these policies and research ethics, we refrained from bypassing such restrictions and instead pursued official authorization for academic evaluation, which was ultimately not granted. Further details regarding our attempts and the corresponding policy constraints are provided in Appendix F.3.

Despite the lack of direct access to commercial APIs, we expect our findings to generalize to such systems. Modern commercial SRSs are typically built upon deep learning-based architectures similar to those evaluated in this work, and our attack relies solely

on score-based feedback without requiring gradient access. Accordingly, even normalized confidence scores commonly returned by commercial APIs can be exploited by score-based optimization methods such as NES. To approximate commercial-grade robustness, we therefore evaluate our attack on strong, publicly available models, including those released by Alibaba's 3D-Speaker group ( $C_1$ ,  $C_2$ ) and NVIDIA ( $T_3$ ).

## 8 Conclusion

In this work, we investigated score-based speaker impersonation attacks under a realistic black-box setting without access to victim voice samples. We show that the primary bottleneck of prior attacks lies not only in the high dimensionality of the audio space, but more fundamentally in the misalignment between the optimization space and speaker-discriminative embedding geometry.

Motivated by this insight, we reformulate score-based impersonation as a black-box optimization problem and identify feature-to-speech inversion as a critical missing component. We propose a feature-aligned inverse model trained via fixed-text fine-tuning with identity and structure constraints, explicitly aligning the latent space with speaker embeddings while preserving identity and cross-model compatibility.

Leveraging this inverse model, we enable two complementary attack paradigms: (i) a query-efficient NES-based attack in the inverse-induced latent space, and (ii) a non-adaptive subspace-projection attack that exploits score-level structural leakage and was previously infeasible. Extensive experiments show that both attacks achieve high success rates with orders-of-magnitude fewer queries than prior approaches and generalize across heterogeneous models and languages.

Overall, our results establish feature-aligned inversion as a key enabler for practical score-based speaker impersonation attacks and demonstrate that exposing similarity scores poses significant security risks, calling for careful system design and stronger defenses in deployed speaker recognition systems.

## Ethical Statement

We attest that we have read the ethics-related discussions in the conference call for papers and the submission guidelines. The authors have considered the ethical implications of this work and believe that the research was conducted responsibly. This work studies speaker impersonation attacks solely for research purposes, with the goal of evaluating the security of speaker recognition systems. We do not conduct attacks against real-world systems. All experiments are performed using publicly available datasets and open-source models. No private or sensitive data is collected, and thus institutional review board (IRB) approval was not required. Details on dataset collection, processing, and access are provided. To mitigate potential misuse, we release only a minimal implementation sufficient to reproduce our experimental results. The released code is intentionally limited and is not designed for direct use against real-world speaker recognition or authentication systems.

## Open Sciences

We provide all the implementation to reproduce our experimental results through the anonymized GitHub link: <https://anonymous.4open.science/r/Scores-Know-Bobs-Voice-5B14>. We release a minimal attack pipeline that is sufficient to validate the correctness of our experimental results. The provided implementation is intentionally scoped for research evaluation and is not designed for direct use against real-world speaker recognition or authentication systems. Our anonymized repository documents how to obtain the publicly available datasets and open-source speaker recognition, text-to-speech models used in our experiments. No proprietary data, trained attack models, or end-to-end attack systems are distributed. The full source code will be made publicly available upon paper acceptance.

## References

- [1] Sohaib Ahmad and Benjamin Fuller. 2020. Resist: Reconstruction of irises from templates. In *2020 IEEE International Joint Conference on Biometrics (IJCB)*. IEEE, 1–10.
- [2] Zahid Akhtar, Christian Micheloni, and Gian Luca Foresti. 2015. Biometric Liveness Detection: Challenges and Research Opportunities. *IEEE Security & Privacy* 13, 5 (2015), 63–72. doi:10.1109/MSP.2015.116
- [3] Moustafa Alzantot, Bharathan Balaji, and Mani Srivastava. 2018. Did you hear that? adversarial examples against automatic speech recognition. *arXiv preprint arXiv:1801.00554* (2018).
- [4] Amazon Web Services. 2024. *Amazon Transcribe - Speaker Identification*. <https://docs.aws.amazon.com/transcribe/latest/dg/speaker-identification.html> Provides confidence scores for identified speaker segments.
- [5] Zhongxin Bai and Xiao-Lei Zhang. 2021. Speaker recognition based on deep learning: An overview. *Neural Networks* 140 (2021), 65–99.
- [6] Philip Bontrager, Aditi Roy, Julian Togelius, Nasir Memon, and Arun Ross. 2018. DeepMasterPrints: Generating MasterPrints for Dictionary Attacks via Latent Variable Evolution. In *2018 IEEE 9th International Conference on Biometrics Theory, Applications and Systems (BTAS)*. 1–9. doi:10.1109/BTAS.2018.8698539
- [7] Edresson Casanova, Kelly Davis, Eren Gölge, Görkem Gökner, Iulian Gulea, Logan Hart, Aya Aljafari, Joshua Meyer, Reuben Morais, Samuel Olayemi, et al. 2024. Xtts: a massively multilingual zero-shot text-to-speech model. *arXiv preprint arXiv:2406.04904* (2024).
- [8] Edresson Casanova, Julian Weber, Christopher D Shulby, Arnaldo Candido Junior, Eren Gölge, and Moacir A Ponti. 2022. Yourtts: Towards zero-shot multi-speaker tts and zero-shot voice conversion for everyone. In *International conference on machine learning*. PMLR, 2709–2720.
- [9] Guangke Chen, Sen Chenb, Lingling Fan, Xiaoning Du, Zhe Zhao, Fu Song, and Yang Liu. 2021. Who is real bob? adversarial attacks on speaker recognition systems. In *2021 IEEE Symposium on Security and Privacy (SP)*. IEEE, 694–711.

- [10] Guangke Chen, Yedi Zhang, Zhe Zhao, and Fu Song. 2023. {QFA2SR}:{Query-Free} Adversarial Transfer Attacks to Speaker Recognition Systems. In *32nd USENIX Security Symposium (USENIX Security 23)*. 2437–2454.
- [11] Guangke Chen, Zhe Zhao, Fu Song, Sen Chen, Lingling Fan, Feng Wang, and Jiashui Wang. 2022. Towards Understanding and Mitigating Audio Adversarial Examples for Speaker Recognition. *IEEE Transactions on Dependable and Secure Computing* (2022).
- [12] Pin-Yu Chen, Huan Zhang, Yash Sharma, Jinfeng Yi, and Cho-Jui Hsieh. 2017. Zoo: Zeroth order optimization based black-box attacks to deep neural networks without training substitute models. In *Proceedings of the 10th ACM workshop on artificial intelligence and security*. 15–26.
- [13] Yafeng Chen, Siqi Zheng, Hui Wang, Luyao Cheng, et al. 2025. 3D-Speaker-Toolkit: An Open Source Toolkit for Multi-modal Speaker Verification and Diarization. (2025).
- [14] Yafeng Chen, Siqi Zheng, Hui Wang, Luyao Cheng, Qian Chen, and Jiajun Qi. 2023. An Enhanced Res2Net with Local and Global Feature Fusion for Speaker Verification. (2023).
- [15] Zesheng Chen. 2023. On the detection of adaptive adversarial attacks in speaker verification systems. *IEEE Internet of Things Journal* 10, 18 (2023), 16271–16283.
- [16] Joon Son Chung, Jaesung Huh, Seongkyu Mun, Minjae Lee, Hee Soo Heo, Soyeon Choe, Chiheon Ham, Sunghwan Jung, Bong-Jin Lee, and Icksang Han. 2020. In defence of metric learning for speaker recognition. In *Proc. Interspeech*. 2977–2981.
- [17] Joon Son Chung, Arsha Nagrani, and Andrew Senior. 2018. Voxceleb2: Deep speaker recognition. *arXiv preprint arXiv:1806.05622* (2018).
- [18] Christopher Cieri, David Miller, and Kevin Walker. 2004. The Fisher Corpus: A Resource for the Next Generations of Speech-to-Text. In *Proceedings of the Fourth International Conference on Language Resources and Evaluation (LREC'04)*, Maria Teresa Lino, Maria Francisca Xavier, Fátima Ferreira, Rute Costa, and Raquel Silva (Eds.). European Language Resources Association (ELRA), Lisbon, Portugal. <https://aclanthology.org/L04-1500/>
- [19] Brecht Desplanques, Jenhe Thienpondt, and Kris Demuynck. 2020. ECAPA-TDNN: Emphasized Channel Attention, Propagation and Aggregation in TDNN Based Speaker Verification. In *Interspeech 2020*. 3830–3834. doi:10.21437/Interspeech.2020-2650
- [20] Tianyu Du, Shouling Ji, Jinfeng Li, Qinchen Gu, Ting Wang, and Raheem Beyah. 2020. Sirenattack: Generating adversarial audio for end-to-end acoustic systems. In *Proceedings of the 15th ACM Asia conference on computer and communications security*. 357–369.
- [21] Chi Nhan Duong, Thanh-Dat Truong, Khoa Luu, Kha Gia Quach, Hung Bui, and Kaushik Roy. 2020. Vec2face: Unveil human faces from their blackbox features in face recognition. In *Proceedings of the IEEE/CVF Conference on Computer Vision and Pattern Recognition*. 6132–6141.
- [22] Gölgel Eren and The Coqui TTS Team. 2021. *Coqui TTS*. doi:10.5281/zenodo.6334862
- [23] Yue Fan, JW Kang, LT Li, KC Li, HL Chen, ST Cheng, PY Zhang, ZY Zhou, YQ Cai, and Dong Wang. 2020. Cn-cele: a challenging chinese speaker recognition dataset. In *ICASSP 2020-2020 IEEE International Conference on Acoustics, Speech and Signal Processing (ICASSP)*. IEEE, 7604–7608.
- [24] J.J. Godfrey, E.C. Holliman, and J. McDaniel. 1992. SWITCHBOARD: telephone speech corpus for research and development. In *Proceedings ICASSP-92: 1992 IEEE International Conference on Acoustics, Speech, and Signal Processing*, Vol. 1. 517–520 vol.1. doi:10.1109/ICASSP.1992.225858
- [25] Chuan Guo, Jacob Gardner, Yurong You, Andrew Gordon Wilson, and Kilian Weinberger. 2019. Simple black-box adversarial attacks. In *International conference on machine learning*. PMLR, 2484–2493.
- [26] Ameer Hamza, Abdul Rehman Rehman Javed, Farkhund Iqbal, Natalia Kryvinska, Ahmad S Almadhor, Zunera Jalil, and Rouba Borghol. 2022. Deepfake audio detection via MFCC features using machine learning. *IEEE Access* 10 (2022), 134018–134028.
- [27] Hee Soo Heo, Bong-Jin Lee, Jaesung Huh, and Joon Son Chung. 2020. Clova baseline system for the voxceleb speaker recognition challenge 2020. *arXiv preprint arXiv:2009.14153* (2020).
- [28] Andrew Ilyas, Logan Engstrom, Anish Athalye, and Jessy Lin. 2018. Black-box adversarial attacks with limited queries and information. In *International conference on machine learning*. PMLR, 2137–2146.
- [29] ISO. 2022. ISO/IEC 24745:2022. Information security, cybersecurity and privacy protection—Biometric information protection.
- [30] Ye Jia, Yu Zhang, Ron Weiss, Quan Wang, Jonathan Shen, Fei Ren, Patrick Nguyen, Ruoming Pang, Ignacio Lopez Moreno, Yonghui Wu, et al. 2018. Transfer learning from speaker verification to multispeaker text-to-speech synthesis. *Advances in neural information processing systems* 31 (2018).
- [31] Sonal Joshi, Saurabh Kataria, Jesús Villalba, and Najim Dehak. 2022. Advest: Adversarial perturbation estimation to classify and detect adversarial attacks against speaker identification. *arXiv preprint arXiv:2204.03848* (2022).
- [32] Zeqian Ju, Yuancheng Wang, Kai Shen, Xu Tan, Detai Xin, Dongchao Yang, Yanqing Liu, Yichong Leng, Kaitao Song, Siliang Tang, et al. 2024. NaturalSpeech 3: Zero-shot speech synthesis with factorized codec and diffusion models. *arXiv preprint arXiv:2403.03100* (2024).
- [33] Jee-weon Jung, You Jin Kim, Hee-Soo Heo, Bong-Jin Lee, Youngki Kwon, and Joon Son Chung. 2022. Pushing the limits of raw waveform speaker recognition. *arXiv preprint arXiv:2203.08488* (2022).
- [34] Christof Kauba, Simon Kirchgasser, Vahid Mirjalili, Andreas Uhl, and Arun Ross. 2020. Inverse biometrics: Reconstructing grayscale finger vein images from binary features. In *2020 IEEE International Joint Conference on Biometrics (IJB/CB)*. IEEE, 1–10.
- [35] Jaehyeon Kim, Jungil Kong, and Juhee Son. 2021. Conditional variational autoencoder with adversarial learning for end-to-end text-to-speech. In *International Conference on Machine Learning*. PMLR, 5530–5540.
- [36] Sunpill Kim, Yong Kiam Tan, Bora Jeong, Soumik Mondal, Khin Mi Mi Aung, and Jae Hong Seo. 2024. Scores Tell Everything about Bob: Non-adaptive Face Reconstruction on Face Recognition Systems. In *2024 IEEE Symposium on Security and Privacy (SP)*. IEEE, 1684–1702.
- [37] Tomi Kinnunen, Rosa González Hautamäki, Ville Vestman, and Md Sahidullah. 2019. Can we use speaker recognition technology to attack itself? enhancing mimicry attacks using automatic target speaker selection. In *ICASSP 2019-2019 IEEE International Conference on Acoustics, Speech and Signal Processing (ICASSP)*. IEEE, 6146–6150.
- [38] Tomi Kinnunen, Md Sahidullah, Héctor Delgado, Massimiliano Todisco, Nicholas Evans, Junichi Yamagishi, and Kong Aik Lee. 2017. The ASVspoof 2017 challenge: Assessing the limits of replay spoofing attack detection. (2017).
- [39] Nithin Rao Koluguri, Taejin Park, and Boris Ginsburg. 2022. Titanet: Neural model for speaker representation with 1d depth-wise separable convolutions and global context. In *ICASSP 2022-2022 IEEE international conference on acoustics, speech and signal processing (ICASSP)*. IEEE, 8102–8106.
- [40] Jungil Kong, Jaehyeon Kim, and Jaekyoung Bae. 2020. Hifi-gan: Generative adversarial networks for efficient and high fidelity speech synthesis. *Advances in neural information processing systems* 33 (2020), 17022–17033.
- [41] Yinghao Aaron Li, Cong Han, Vinay Raghavan, Gavin Mischler, and Nima Mesgarani. 2023. Styletts 2: Towards human-level text-to-speech through style diffusion and adversarial training with large speech language models. *Advances in Neural Information Processing Systems* 36 (2023), 19594–19621.
- [42] Yuke Lin, Ming Cheng, Fulin Zhang, Yingying Gao, Shilei Zhang, and Ming Li. 2024. VoxBlink2: A 100K+ Speaker Recognition Corpus and the Open-Set Speaker-Identification Benchmark. arXiv:2407.11510 [eess.AS] <https://arxiv.org/abs/2407.11510>
- [43] Tianchi Liu, Ivan Kukanov, Zihan Pan, Qiongqiong Wang, Hardik B Sailor, and Kong Aik Lee. 2024. Towards quantifying and reducing language mismatch effects in cross-lingual speech anti-spoofing. In *2024 IEEE Spoken Language Technology Workshop (SLT)*. IEEE, 1185–1192.
- [44] Tianchi Liu, Kong Aik Lee, Qiongqiong Wang, and Haizhou Li. 2023. Disentangling voice and content with self-supervision for speaker recognition. In *Thirty-seventh Conference on Neural Information Processing Systems (NeurIPS)*, Vol. 36. 50221–50236.
- [45] Tianchi Liu, Duc-Tuan Truong, Rohan Kumar Das, Kong Aik Lee, and Haizhou Li. 2025. Nes2Net: A Lightweight Nested Architecture for Foundation Model Driven Speech Anti-spoofing. *arXiv preprint arXiv:2504.05657* (2025).
- [46] Panpan Lu, Qi Li, Hui Zhu, Giuliano Sovernigo, and Xiaodong Lin. 2021. Voxstructor: Voice reconstruction from voiceprint. In *Information Security: 24th International Conference, ISC 2021, Virtual Event, November 10–12, 2021, Proceedings 24*. Springer, 374–397.
- [47] Guangcan Mai, Kai Cao, Pong C Yuen, and Anil K Jain. 2018. On the reconstruction of face images from deep face templates. *IEEE transactions on pattern analysis and machine intelligence* 41, 5 (2018), 1188–1202.
- [48] Microsoft. 2024. *Speaker Recognition API - Cognitive Services*. <https://learn.microsoft.com/en-us/azure/ai-services/speech-service/speaker-recognition-overview> Explicitly returns confidence scores to support adjustable security thresholds.
- [49] Ananda Garin Mills, Patthranit Kaewcharuay, Pannathorn Sathirasattayanon, Suradej Duangpummet, Kasorn Galajit, Jessada Karnjana, and Pakinee Aimmanee. 2022. Replay attack detection based on voice and non-voice sections for speaker verification. In *2022 Asia-Pacific Signal and Information Processing Association Annual Summit and Conference (APSIPA ASC)*. IEEE, 221–226.
- [50] A. Nagrani, J. S. Chung, and A. Zisserman. 2017. VoxCeleb: a large-scale speaker identification dataset. In *INTERSPEECH*.
- [51] National Institute of Standards and Technology. 2008. *The NIST Year 2008 Speaker Recognition Evaluation Plan*. Technical Report. National Institute of Standards and Technology, Gaithersburg, MD, USA. Available: <https://www.nist.gov/document/sre08evalplanrelease4pdf>.
- [52] Huy H Nguyen, Trung-Nghia Le, Junichi Yamagishi, and Isao Echizen. 2023. Analysis of master vein attacks on finger vein recognition systems. In *Proceedings of the IEEE/CVF Winter Conference on Applications of Computer Vision*. 1900–1908.
- [53] NVIDIA. 2023. Overview of Zero-Shot Multi-Speaker TTS Systems: Top Q&As. Speech AI Summit. <https://developer.nvidia.com/blog/overview-of-zero-shot-multi-speaker-tts-systems-top-qas/>.

- [54] Aaron van den Oord, Sander Dieleman, Heiga Zen, Karen Simonyan, Oriol Vinyals, Alex Graves, Nal Kalchbrenner, Andrew Senior, and Koray Kavukcuoglu. 2016. Wavenet: A generative model for raw audio. *arXiv preprint arXiv:1609.03499* (2016).
- [55] Mohamed Osman. 2022. Emo-tts: Parallel transformer-based text-to-speech model with emotional awareness. In *2022 5th International Conference on Computing and Informatics (ICCI)*. IEEE, 169–174.
- [56] OWASP Foundation. 2019. *OWASP API Security Top 10: API3:2019 Excessive Data Exposure*. Technical Report. OWASP. <https://owasp.org/www-project-api-security/highlights-that-api-endpoints-often-expose-full-data-objects-relying-on-client-side-filtering>.
- [57] OWASP Mobile Security Project. 2023. *OWASP Mobile Security Testing Guide (MSTG)*. OWASP Foundation. Describes testing procedures for local authentication using function hooking and dynamic binary instrumentation.
- [58] Sushanta K Pani, Anurag Chowdhury, Morgan Sandler, and Arun Ross. 2023. Voice Morphing: Two Identities in One Voice. In *2023 International Conference of the Biometrics Special Interest Group (BIOSIG)*. IEEE, 1–6.
- [59] Adam Paszke, Sam Gross, Francisco Massa, Adam Lerer, James Bradbury, Gregory Chanan, Trevor Killeen, Zeming Lin, Natalia Gimelshein, Luca Antiga, Alban Desmaison, Andreas Kopf, Edward Yang, Zachary DeVito, Martin Raison, Alykhan Tejani, Sasank Chilamkurthy, Benoit Steiner, Lu Fang, Junjie Bai, and Soumith Chintala. 2019. PyTorch: An Imperative Style, High-Performance Deep Learning Library. In *Advances in Neural Information Processing Systems 32*. Curran Associates, Inc., 8024–8035. <http://papers.neurips.cc/paper/9015-pytorch-an-imperative-style-high-performance-deep-learning-library.pdf>
- [60] Alessandro Pianese, Davide Cozzolino, Giovanni Poggi, and Luisa Verdoliva. 2022. Deepfake audio detection by speaker verification. In *2022 IEEE International Workshop on Information Forensics and Security (WIFS)*. IEEE, 1–6.
- [61] Wei Ping, Kainan Peng, Andrew Gibiansky, Sercan O Arik, Ajay Kannan, Sharan Narang, Jonathan Raiman, and John Miller. 2017. Deep voice 3: Scaling text-to-speech with convolutional sequence learning. *arXiv preprint arXiv:1710.07654* (2017).
- [62] Xiaoyi Qin, Na Li, Chao Weng, Dan Su, and Ming Li. 2022. Simple attention module based speaker verification with iterative noisy label detection. In *ICASSP 2022-2022 IEEE International Conference on Acoustics, Speech and Signal Processing (ICASSP)*. IEEE, 6722–6726.
- [63] Mirco Ravanelli, Titouan Parcollet, Peter Plantinga, Aku Rouhe, Samuele Cornell, Loren Lugosch, Cem Subakan, Nauman Dawalatabad, Abdelwahab Heba, Jianyuan Zhong, Ju-Chieh Chou, Sung-Lin Yeh, Szu-Wei Fu, Chien-Feng Liao, Elena Rastorgueva, François Grondin, William Aris, Hwidong Na, Yan Gao, Renato De Mori, and Yoshua Bengio. 2021. SpeechBrain: A General-Purpose Speech Toolkit. *arXiv:2106.04624 [eess.AS]* <https://arxiv.org/abs/2106.04624>
- [64] Anton Razzhigaev, Klim Kireev, Edgar Kaziakhmedov, Nurislam Tursynbek, and Aleksandr Petiushko. 2020. Black-box face recovery from identity features. In *European Conference on Computer Vision*. Springer, 462–475.
- [65] Yi Ren, Chenxu Hu, Xu Tan, Tao Qin, Sheng Zhao, Zhou Zhao, and Tie-Yan Liu. 2020. FastSpeech 2: Fast and high-quality end-to-end text to speech. *arXiv preprint arXiv:2006.04558* (2020).
- [66] Jonathan Shen, Ruoming Pang, Ron J Weiss, Mike Schuster, Navdeep Jaitly, Zongheng Yang, Zhifeng Chen, Yu Zhang, Yuxuan Wang, Rj Skerrv-Ryan, et al. 2018. Natural tts synthesis by conditioning wavenet on mel spectrogram predictions. In *2018 IEEE international conference on acoustics, speech and signal processing (ICASSP)*. IEEE, 4779–4783.
- [67] David Snyder, Daniel Garcia-Romero, Gregory Sell, Daniel Povey, and Sanjeev Khudanpur. 2018. X-Vectors: Robust DNN Embeddings for Speaker Recognition. In *2018 IEEE International Conference on Acoustics, Speech and Signal Processing (ICASSP)*. 5329–5333. doi:10.1109/ICASSP.2018.8461375
- [68] Hemlata Tak, Massimiliano Todisco, Xin Wang, Jee-weon Jung, Junichi Yamagishi, and Nicholas Evans. 2022. Automatic speaker verification spoofing and deepfake detection using wav2vec 2.0 and data augmentation. *arXiv preprint arXiv:2202.12233* (2022).
- [69] Massimiliano Todisco, Xin Wang, Ville Vestman, Md Sahidullah, Héctor Delgado, Andreas Nautsch, Junichi Yamagishi, Nicholas Evans, Tomi Kinnunen, and Kong Aik Lee. 2019. ASvspoof 2019: Future horizons in spoofed and fake audio detection. *arXiv preprint arXiv:1904.05441* (2019).
- [70] Edward Vendrow and Joshua Vendrow. 2021. Realistic face reconstruction from deep embeddings. In *NeurIPS 2021 Workshop Privacy in Machine Learning*.
- [71] Paul Voigt and Axel Von dem Bussche. 2017. The eu general data protection regulation (gdpr). *A practical guide, 1st ed.*, Cham: Springer International Publishing 10, 3152676 (2017), 10–5555.
- [72] Li Wan, Quan Wang, Alan Papir, and Ignacio Lopez Moreno. 2018. Generalized end-to-end loss for speaker verification. In *2018 IEEE International Conference on Acoustics, Speech and Signal Processing (ICASSP)*. IEEE, 4879–4883.
- [73] Hongji Wang, Chengdong Liang, Shuai Wang, Zhengyang Chen, Binbin Zhang, Xu Xiang, Yanlei Deng, and Yanmin Qian. 2023. Wespeaker: A research and production oriented speaker embedding learning toolkit. In *ICASSP 2023-2023 IEEE International Conference on Acoustics, Speech and Signal Processing (ICASSP)*. IEEE, 1–5.
- [74] Hui Wang, Siqi Zheng, Yafeng Chen, Luyao Cheng, and Qian Chen. 2023. CAM++: A Fast and Efficient Network for Speaker Verification Using Context-Aware Masking. (2023).
- [75] Kun Wang, Xiangyu Xu, Li Lu, Zhongjie Ba, Feng Lin, and Kui Ren. 2024. {FraudWhistler}: A Resilient, Robust and Plug-and-play Adversarial Example Detection Method for Speaker Recognition. In *33rd USENIX Security Symposium (USENIX Security 24)*. 7303–7320.
- [76] Shuai Wang, Zhengyang Chen, Kong Aik Lee, Yanmin Qian, and Haizhou Li. 2024. Overview of Speaker Modeling and Its Applications: From the Lens of Deep Speaker Representation Learning. *IEEE/ACM Transactions on Audio, Speech, and Language Processing* 32 (2024), 4971–4998. doi:10.1109/TASLP.2024.3492793
- [77] Xin Wang, Héctor Delgado, Hemlata Tak, Jee-weon Jung, Hye-jin Shim, Massimiliano Todisco, Ivan Kukanov, Xuechen Liu, Md Sahidullah, Tomi Kinnunen, et al. 2024. ASvspoof 5: Crowdsourced speech data, deepfakes, and adversarial attacks at scale. *arXiv preprint arXiv:2408.08739* (2024).
- [78] Daan Wierstra, Tom Schaul, Tobias Glasmachers, Yi Sun, Jan Peters, and Jürgen Schmidhuber. 2014. Natural evolution strategies. *The Journal of Machine Learning Research* 15, 1 (2014), 949–980.
- [79] Kanishka P Wijewardena, Steven A Grosz, Kai Cao, and Anil K Jain. 2022. Fingerprint template invertibility: Minutiae vs. deep templates. *IEEE Transactions on Information Forensics and Security* 18 (2022), 744–757.
- [80] Haibin Wu, Po-Chun Hsu, Ji Gao, Shanshan Zhang, Shen Huang, Jian Kang, Zhiyong Wu, Helen Meng, and Hung-Yi Lee. 2022. Adversarial sample detection for speaker verification by neural vocoders. In *ICASSP 2022-2022 IEEE international conference on acoustics, speech and signal processing (ICASSP)*. IEEE, 236–240.
- [81] Ivan Yakovlev, Rostislav Makarov, Andrei Balykin, Pavel Malov, Anton Okhotnikov, and Nikita Torgashov. 2024. Reshape Dimensions Network for Speaker Recognition. In *Interspeech 2024*. 3235–3239. doi:10.21437/Interspeech.2024-2116
- [82] Junichi Yamagishi, Xin Wang, Massimiliano Todisco, Md Sahidullah, Jose Patino, Andreas Nautsch, Xuechen Liu, Kong Aik Lee, Tomi Kinnunen, Nicholas Evans, et al. 2021. ASvspoof 2021: accelerating progress in spoofed and deepfake speech detection. *arXiv preprint arXiv:2109.00537* (2021).
- [83] Licheng Yan, Fei Wang, Lu Leng, and Andrew Beng Jin Teoh. 2024. Toward comprehensive and effective palmprint reconstruction attack. *Pattern Recognition* 155 (2024), 110655.
- [84] Sung-Hyun Yoon, Min-Sung Koh, Jae-Han Park, and Ha-Jin Yu. 2020. A new replay attack against automatic speaker verification systems. *IEEE Access* 8 (2020), 36080–36088.
- [85] Baolin Zheng, Peipei Jiang, Qian Wang, Qi Li, Chao Shen, Cong Wang, Yunjie Ge, Qingyang Teng, and Shenyi Zhang. 2021. Black-box adversarial attacks on commercial speech platforms with minimal information. In *Proceedings of the 2021 ACM SIGSAC conference on computer and communications security*. 86–107.
- [86] Jincheng Zhou, Tao Hai, Dayang NA Jawawi, Dan Wang, Ebuka Ibeke, and Cresantus Biamba. 2022. Voice spoofing countermeasure for voice replay attacks using deep learning. *Journal of Cloud Computing* 11, 1 (2022), 51.
- [87] Chu-Xiao Zuo, Zhi-Jun Jia, and Wu-Jun Li. 2024. AdvTTS: Adversarial Text-to-Speech Synthesis Attack on Speaker Identification Systems. In *ICASSP 2024-2024 IEEE International Conference on Acoustics, Speech and Signal Processing (ICASSP)*. IEEE, 4840–4844.

## A Additional Related Works

Various threats and attack scenarios have been proposed for speaker recognition systems (SRSs) ranging from compromising their training data to physical attacks against deployed systems. Given the broad range of threats, we will primarily focus our related work discussion on the *impersonation attack* setting, where an attacker presents an attack sample in order to impersonate an identity enrolled in the targeted SRS. A summary of prior research on speaker impersonation is shown in Table 8; as can be seen from the table, there are numerous impersonation vulnerabilities in SRSs through attacks with diverse assumptions and methodologies.

*Known-Victim and Physical Attacks.* One prominent line of research operates under the assumption that the attacker has direct access to the victim’s voice samples or related information. This category includes attacks involving human voice mimicry [37], replay attacks using recorded speech [84], or voice synthesis methods that generate speech recognized as identical to two identities simultaneously [58]. While these methods share the functionality of attempting impersonation based on prior information, they differ in their specific objectives and execution, ranging from direct human performance and simple playback to the computational generation of ambiguous, multi-identity audio.

*Generative and Transfer Attacks.* Other studies have attempted to generate victim voices by leveraging knowledge about the targeted system or through more complex interactions. For instance, the voice synthesis approach of Jia et al. [30] operates in a white-box setting, utilizing internal model information to generate speech recognized as a specific identity. In contrast, Voxstructor [46] targets black-box models but requires performing an extensive number ( $\geq 100K$ ) of non-adaptive queries to reconstruct the victim’s feature vector, which is then used to train a separate model for generating the target voice. Notably, Voxstructor requires *feature vector* queries from the black-box SRS, which is challenging to apply against deployed systems because such vectors are usually carefully stored as private user biometric data. Transfer-based attack strategies have also been explored, which utilize victim information during preparation but do not directly query the target model during the attack phase. AdvTTS [87], for example, trained a model to generate adversarial noise that causes a source audio sample to be recognized as a target audio sample. QFA2SR [10] enhanced their transferability to black-box environments using ensemble techniques involving multiple surrogate models.

*Black-Box Attacks.* Black-box attacks involve making queries to the target model SRS, but often require some pre-existing victim voice information and predominantly rely on adaptive query strategies. Representative examples include SirenAttack [20], which generates adversarial samples based on score feedback through approximately 7,500 adaptive queries; and Occam [85], which optimizes attacks based on decision feedback using around 10K adaptive queries. These methods employ gradual attack refinement based on query feedback and necessitate a substantial number of queries. The closest work to our paper’s setting is FakeBob [9], which performs black-box impersonation attacks via score queries without prior victim voice information. Their work demonstrated the feasibility of score-based attacks with no *a priori* information of the victim.

However, it relies on an adaptive query strategy and requires a relatively large number of queries ( $\geq 10K$ ) for successful impersonation. We provide a comprehensive comparison using FakeBob against state-of-the-art SRS models in Section 6.

*Countermeasures.* Alongside the emerging impersonation attacks, several countermeasures have been proposed to mitigate them, including the ASVspoof challenges [38, 69, 77, 82]. A widely-used defense strategy against impersonation attacks is to deploy attack detectors, e.g., replay attack detection [49, 86], deepfake detection [26, 45, 60, 68], and adversarial attack detection [15, 31, 75, 80]. In particular, [15] is noteworthy as a detection technique specialized in adaptive query-based attacks, such as Fakebob [9].

*Non-Adaptive Attack on Face Recognition.* A non-adaptive attack that can independently and simultaneously generate all attack queries without any prior information was recently proposed in the domain of face recognition by Kim et al. [36]. A key observation of their work is that the similarity scores which are output by two well-trained face recognition models  $A$  and  $B$  should be similar. Thus, if one can obtain queried scores from a target model  $B$ , then reconstruction can be carried out by transferring those scores to a local model  $A$  and using a so-called inverse model  $A^{-1}$  that reverses the image-to-feature mapping of  $A$ . They demonstrate successful attacks against commercial and open-source targets using only 100 similarity scores obtained via non-adaptive queries. Our work investigates, for the first time, how ideas from this prior attack can be deployed against speaker recognition systems. Notably, the adaptation is not straightforward—unlike face recognition, there is no effective technique to obtain a neural network which acts as the inverse function of an arbitrary speaker recognition model. We remark that if an attacker can make an unlimited number of queries, there have been several approaches [21, 47] to train an inverse neural network by obtaining pseudo-labels, e.g., feature vectors, for all the facial image data that the attacker has. However, these approaches require an enormous number ( $\geq 1M$ ) of feature vector queries, which we consider to be impractical.

## B Additional Description of Inverse Models on Speaker Recognition

In this section, we provide (1) the candidate selection for inverse models used for comparison in the main paper, (2) implementation details of the selected candidates, (3) technical challenges of building custom inverse models, and (4) alternatives for inverse models.

### B.1 Use of Existing TTS Models as Inverse Model Candidates

In designing our attack methodology, the selection of an effective inverse model (responsible for generating audio from a speaker embedding and text) is crucial. While our main experiments in Table 4 compared the proposed method against selected zero-shot TTS (ZS-TTS) baselines, our initial investigation considered a wider array of contemporary Text-to-Speech (TTS) models as potential candidates for this role. A key requirement for a TTS model to function as a suitable inverse model within our specific attack framework in Figure 9 is its ability to generate audio conditioned

**Table 8: Comparison of prior attack methods enabling speaker impersonation against SRSs, summarizing their methodologies, requirements (victim voice, target model access), and query strategies. The details of FakeBob are given for its *speaker verification* setting, which we denote as FakeBob<sup>†</sup> in this table.**

Method	Impersonation Type	Target Model	Victim’s Voice Requirement	Strategy	Query to Target Model	
					Output Format	Number
[37]	Voice Mimicry	Black-box	○	Human Mimicry	-	0
[84]	Replay Attack	Black-box	○	Playback	-	0
[58]	Voice Morphing	Black-box	○	Identity Morphing	-	0
SV2TTS [30]	Speech Synthesis	White-box	○	Training-based	-	0
Voxstructor [46]	Speech Synthesis	Black-box	○	Training-based	Feature vector	≥ 100K
AdvTTS [87]	Adversarial Example	Black-box	○	Transfer-based	-	0
QFA2SR [10]	Adversarial Example	Black-box	○	Transfer-based	-	0
SirenAttack [20]	Adversarial Example	Black-box	○	Adaptive Query	Score	≥ 7500
Occam [85]	Adversarial Example	Black-box	○	Adaptive Query	Decision	≥ 10K
FakeBob <sup>†</sup> [9]	Adversarial Example	Black-box	×	Adaptive Query	Score	≥ 10K
<b>Ours-NES</b>	<b>Speech Synthesis</b>	<b>Black-box</b>	×	<b>Adaptive Query</b>	<b>Score</b>	<b>≈ 500</b>
<b>Ours-SP</b>	<b>Speech Synthesis</b>	<b>Black-box</b>	×	<b>Non-Adaptive Query</b>	<b>Score</b>	<b>50</b>

solely on a target speaker embedding and a predefined text, without requiring additional inputs like a reference audio sample.

We evaluated several prominent TTS architectures based on this criterion. However, many state-of-the-art TTS systems, while powerful for synthesis, do not meet this specific requirement, rendering them unsuitable for direct use as the inverse model in our attack pipeline. Table 9 provides details on some of these considered but ultimately unselected TTS candidates, summarizing their input requirements and inherent limitations for our purpose.

Models like Tacotron2 [66] and FastSpeech2 [65] are not designed to accept speaker embeddings or feature vectors as conditioning input for speaker identity control. Another group of models, including advanced ZS-TTS systems like XTTS [7], EmoTTS [55], NaturalSpeech3 [32], and StyleTTS2 [41], necessitate a reference voice sample during inference. This sample is used by their respective encoders to extract auxiliary acoustic information (such as style, prosody, timbre details, etc.) beyond just the core speaker identity represented by a standard embedding. Since our attack scenario presupposes access only to the target speaker embedding (not a full voice sample), these models cannot generate the required audio output based solely on the embedding and text, thus disqualifying them as inverse model candidates for our study. The above consideration justifies our focus on the models evaluated in our main paper’s comparison and the development of our proposed inversion approach.

## B.2 Additional Details of Selected ZS-TTS Inverse Model Candidates

This section details the specific implementations and configurations used for the chosen inverse model candidates evaluated in our main comparisons: SV2TTS, Voxstructor, and YourTTS. These models were configured to accept a speaker embedding and text as input to generate audio, simulating their role as potential inversion mechanisms.

*SV2TTS [30].* This model adapts the Tacotron2 [66] architecture for zero-shot voice conversion. The primary modification relevant

to its use as an inverse model is that its encoder takes the concatenation of text embeddings and a speaker embedding as input. It generates a mel-spectrogram, which is then converted to a waveform using a pre-trained WaveNet vocoder [54]. For our experiments, we utilized the official implementation provided by the authors.

*Voxstructor [46].* This model was proposed as a method to adapt SV2TTS for use with arbitrary black-box speaker encoders, through the introduction of a mapping layer which transforms the embedding from a target speaker encoder into the GE2E [72] embedding space used internally by SV2TTS. Since no official implementation was readily available that matched our specific target encoder choice, we implemented and trained the Voxstructor mapping component ourselves. Specifically, we designated RawNet3 [33] as the representative black-box target encoder. The mapping layer was constructed using three fully connected layers, each followed by Batch Normalization and a ReLU activation function. We trained this mapping layer for 80 epochs on the VoxCeleb1 trainset, using the Smooth L1 loss between the mapped RawNet3 embeddings and the corresponding ground-truth GE2E embeddings. The Adam optimizer was used with a learning rate of 0.001. The rest of the SV2TTS architecture (decoder and vocoder) remained the same as the original SV2TTS implementation.

*YourTTS [8].* This model is based on the VITS [35] architecture, incorporating modifications for improved zero-shot TTS. It employs a Transformer-based text encoder, takes a speaker embedding as input for conditioning, utilizes a stochastic duration predictor for alignment, and generates the final waveform using a flow-based decoder followed by a HiFi-GAN vocoder [40]. For our evaluation, we employed the implementation available in Coqui.

*Statistics for ZS-TTS ID-Constraint Evaluation.* This section provides the detailed statistical data (mean ± standard deviation) corresponding to the score histograms presented in Figure 1, which evaluate the suitability of standard Zero-Shot Text-to-Speech (ZS-TTS) models as direct inverse models. Table 10 lists these statistics for Positive, Negative, and ID-constraints scores across representative

**Table 9: Other considered TTS models for Inverse Model Candidates.**

TTS	Input	(Speaker) Encoder	Auxiliary Input	Output
Tacotron2 [66]	Text	None	None	Mel-spectrogram Waveform
FastSpeech2 [65]	Text	None	None	Mel-spectrogram Waveform
XTTS [7]	Text, Voice Sample	H/ASP [27], Perceiver Conditioner	Speaker Feature Vector Identity, Style, Prosody, etc.	Waveform
EmoTTS [55]	Text, Voice Sample	SER model (based on Deep Voice3 [61])	Emotion, Speaker Embedding	Mel-spectrogram
NaturalSpeech3 [32]	Text, Voice Sample	Convolutional Blocks	Content, Prosody, Timbre, Acoustic Details	Waveform
StyleTTS2 [41]	Text, Voice Sample	Acoustic and Prosodic, Style Encoders	Style Embedding	Waveform

**Table 10: ID-constraint test statistics for selected ZS-TTS on VoxCeleb1 test dataset.**

Scores	SV2TTS	Voxstructor	YourTTS
Pos.	$0.7795 \pm 0.0771$	$0.6470 \pm 0.1212$	$0.6549 \pm 0.1007$
Neg.	$0.5766 \pm 0.0707$	$0.0267 \pm 0.1119$	$0.1383 \pm 0.1095$
ID-const.	$0.6944 \pm 0.0761$	$0.0472 \pm 0.0879$	$0.4015 \pm 0.0923$

ZS-TTS models (SV2TTS, Voxstructor, YourTTS) on the VoxCeleb1 testset.

The key ID-constraints scores for the ZS-TTS models quantitatively support the visual observation from Fig. 1. These values highlight the significant gap compared to ideal identity preservation (represented by Positive scores) and confirm the limitations of using these off-the-shelf ZS-TTS models directly for high-fidelity speaker embedding inversion as required in our attack context.

## C Additional Experimental Details on ID-Constraints and Transferability

This appendix provides implementation details and complete experimental results for the *ID-Constraints Test* and its *transferability variant*, which are only briefly described in the main paper. All quantitative results omitted from the main text are fully reported in Figure 8.

### C.1 ID-Constraints Test

The ID-Constraints Test evaluates whether the inverse model  $F^{-1}$  preserves speaker identity when performing a round-trip mapping from audio to speaker embedding and back to audio. Given a speaker recognition (SR) feature extractor  $F : \mathcal{A} \rightarrow \mathbb{S}^{d-1}$  and its corresponding inverse model  $F^{-1} : \mathbb{S}^{d-1} \times \mathcal{T} \rightarrow \mathcal{A}$ .

Concretely, for an input utterance *aud*, we first extract its speaker embedding  $x = F(\text{aud})$ . We then synthesize a new audio sample using the inverse model conditioned on a predefined text prompt *Text*, and re-extract its embedding via the same SR model. Identity preservation is quantified by the cosine similarity  $s = \langle x, x' \rangle$  between the original and reconstructed embeddings.

*Experimental setup.* The test is conducted on the VoxCeleb1 test set, consisting of 4,708 utterances from 40 distinct identities. For all zero-shot TTS (ZS-TTS) models, the text prompt is fixed to: “Hello Google, Hi Bixby, Hey Siri”. This ensures that variations in linguistic content do not confound identity evaluation.

*Reference distributions.* To contextualize the ID-Constraints scores, we additionally compute: (i) *positive scores*, obtained from pairs of utterances belonging to the same identity, and (ii) *negative scores*, obtained from utterances of different identities. These distributions serve as upper and lower reference bounds, respectively.

### C.2 Transfer ID-Constraints Test

While the basic ID-Constraints Test evaluates identity preservation under the same SR model used to extract the conditioning embedding, it does not capture cross-model generalization.

In this setting, the inverse model  $F^{-1}$  is instantiated with a local SR model  $F$ , while identity preservation is evaluated using a distinct test-time SR extractor  $F_{\text{test}} : \mathcal{A} \rightarrow \mathbb{S}^{d-1}$ . Importantly,  $F_{\text{test}}$  may differ architecturally and parametrically from  $F$ , reflecting a more realistic scenario in which the attacker does not know the target system.

Given an utterance *aud*, we compute  $x = F_{\text{test}}(\text{aud})$  and  $\tilde{x} = F_{\text{test}}(F^{-1}(F(\text{aud}), \text{Text}))$ , and report their cosine similarity. A high similarity score indicates that the identity information injected by  $F^{-1}$  generalizes beyond the local SR model used during inversion.

### C.3 Complete Results

Figure 8 presents the full distributions of similarity scores for all evaluated systems and test-time extractors  $\{F_T\}_{T=1}^5$ . For each  $F_T$ , we report: (i) positive reference distributions (blue), (ii) negative reference distributions (orange), and (iii) round-trip ID-Constraints scores under transfer conditions (red).

All quantitative findings related to identity preservation and transferability are contained in this figure. The main paper focuses on high-level trends and implications, while detailed distributional behaviors and cross-model comparisons are deferred to this appendix for completeness.

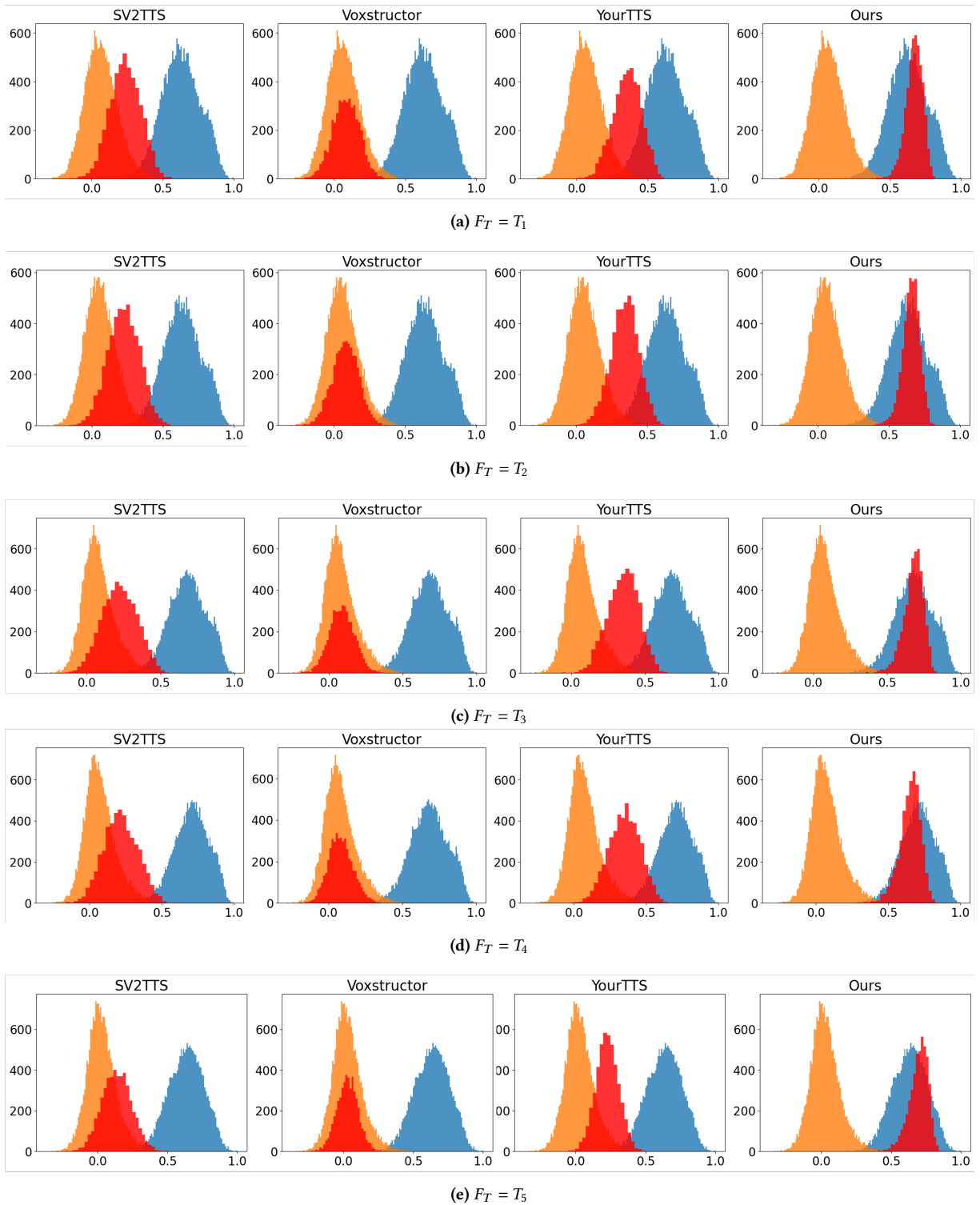


**Figure 8: Distributions of round-trip similarity scores  $s_T(v)$  (red) evaluated on the each  $F_T$ . Positive (blue) and negative (orange) reference distributions are shown for comparison.**

## D Additional Experiment Setup and Implementation Details

In this section, we provide a detailed description of the experimental setup and implementation details used throughout this study. Specifically, we elaborate on the following components: (1) the evaluation metrics for speaker recognition performance, (2) the fine-tuning procedure employed for training the inverse model, including the setup of trainable parameters for fine-tuning and construction of  $\delta$ -OVS, (3) the configuration of both the target models and the local surrogate models utilized for executing the proposed attack, and (4) the implementation details of FakeBob.

### D.1 Evaluation Metrics

For evaluation of speaker recognition, common metrics include the Equal Error Rate (EER) and the minimum Detection Cost Function (minDCF); EER is the error rate at which the False Acceptance Rate (FAR) and the False Rejection Rate (FRR) are equal; minDCF is a cost-based metric widely used in practical applications, particularly in the annual speaker recognition challenge held by NIST [51]. According to the official evaluation plan, one commonly used parameter setting in the audio track is id:1, which corresponds to  $P_{\text{target}} = 0.01$ ,  $C_{\text{FalseAlarm}} = C_{\text{Miss}} = 1$ . Both metrics can be expressed in terms of FAR and FRR, where  $\text{FRR}(\tau) = 1 - \text{TAR}(\tau)$ , as follows:

$$\text{EER} = \frac{\text{FRR}(\hat{\tau}) + \text{FAR}(\hat{\tau})}{2},$$

$$\text{where } \hat{\tau} = \arg \min_{\tau} |\text{FAR}(\tau) - \text{FRR}(\tau)|.$$

$$\begin{aligned} \text{minDCF} = \min_{\tau} & \left( C_{\text{miss}} \cdot \text{FRR}(\tau) \cdot (1 - P_{\text{target}}) \right. \\ & \left. + C_{\text{FalseAlarm}} \cdot \text{FAR}(\tau) \cdot P_{\text{target}} \right). \end{aligned}$$

As these definitions suggest, lower EER and minDCF indicate better discrimination ability, meaning the model performs more effectively in distinguishing speakers.

### D.2 Experiment and Implementation Details

All experiments were performed on a single NVIDIA A100 GPU using PyTorch [59] and SpeechBrain [63]. Full utterances were used for all inferences. In addition, when using open source speaker recognition systems (SRS), the official inference codes provided by each model were utilized.

**D.2.1 Fine-Tuning an Inverse Model (EN).** We used YourTTS as the foundation for our local inverse model (implementation provided by Coqui [22]). To apply our fine-tuning technique, we used the training set of VoxCeleb1 [50] with a batch size of 64, and the gradient accumulation step set at 4. Also,  $\lambda_{\text{IC}} = 5$  and  $\lambda_{\text{SC}} = 1$ . We employed AdamW as the optimizer, and the learning rate was gradually lowered from 1e-3 to 1e-5 via CosineAnnealing scheduling.

**D.2.2 Fine-Tuning an Inverse Model (CN).** We used YourTTS as the foundation for our local inverse model (implementation provided by Coqui [22]). To apply our fine-tuning technique, we used the training set of CNCeleb1,2 [23]. To bridge the dimensionality gap between the output of  $L_{\text{CN}}$  (256) and the YourTTS speaker encoder (512), we integrated a residual *LinkBlock* consisting of linear projections, LayerNorm, and GELU activation. This block is trained

end-to-end, with the SC loss applied between its input and output to preserve the topological structure of the feature space. The training settings included a batch size of 64, a gradient accumulation step of 4,  $\lambda_{\text{IC}} = 5$ , and  $\lambda_{\text{SC}} = 1$ . We employed AdamW as the optimizer, with the learning rate gradually lowered from 1e-3 to 1e-5 via CosineAnnealing scheduling.

**D.2.3 Parameter Configuration for Inverse Model Fine-Tuning.** This paragraph provides further details on the specific parameter configuration used when fine-tuning the pre-trained YourTTS model [8] to act as our inverse model  $F^{-1}$ , as mentioned in Sec. 5.3. The goal is to leverage the fixed-text strategy and focus the learning process on adapting the model to generate audio  $\widetilde{\text{aud}}_i$  that reflects the input speaker embedding  $F(\text{aud}_i)$ , while preserving the linguistic quality derived from the fixed input text *Text*.

YourTTS builds upon the VITS architecture [35] and comprises several interconnected modules. Our fine-tuning strategy focuses learning by selectively freezing specific components related to the fixed input text. Specifically, the Text Encoder, responsible for converting the input text *Text* into linguistic representations (including any associated Language Embeddings if applicable for the specific pre-trained model), is kept entirely frozen. Since the text input and its corresponding language are constant in our setup, preserving the pre-trained text and language representations is crucial for maintaining linguistic consistency. Similarly, the Duration Predictor, which predicts the duration for each linguistic unit based on the text content, is also kept frozen to maintain the prosodic structure associated with the fixed input text. The Posterior Encoder, a VITS component primarily used during training, is less critical for adaptation in this context as our focus is on the prior pathway driven by the speaker embedding.

Conversely, the core generative pathway, encompassing the prior encoder, decoder, and normalizing flow, is made trainable. This pathway is responsible for synthesizing the output Mel-spectrogram conditioned on the linguistic representations, predicted durations, and, critically, the input speaker embedding  $F(\text{aud}_i)$ . Making these components trainable allows the model to learn the crucial mapping from the speaker embedding  $F(\text{aud}_i)$  to the corresponding vocal characteristics needed for generating  $\widetilde{\text{aud}}_i$ . The gradient updates originating from our specialized loss functions in Section 5.2 primarily influence these parameters, adjusting how the model synthesizes the Mel-spectrogram according to the target speaker identity.

Furthermore, the parameters of the vocoder (e.g., HiFi-GAN), which transforms the generated Mel-spectrogram into the final waveform  $\widetilde{\text{aud}}_i$ , are also made trainable in our approach. Fine-tuning the vocoder allows the waveform generation process itself to adapt to the target speaker identity and the fine-tuning objective. This potentially enables the model to capture finer acoustic details directly at the waveform synthesis stage, further enhancing the identity preservation driven by our loss functions.

In summary, by freezing the text-related components (text Encoder, including language aspects, and duration predictor), we concentrate the fine-tuning updates on the core acoustic model responsible for Mel-spectrogram generation conditioned on  $F(\text{aud}_i)$ , as well as the vocoder responsible for the final waveform synthesis. This targeted approach aims to maximize the model’s adaptation

**Table 11: Hyperparameters for Audio-NES**

Hyperparameter	Value
Search variable	waveform $\text{aud} \in \mathbb{R}^{48000}$
Initialization	$\mathcal{N}(0, I_{48000})$
Candidate pool size $C$	100
Selected candidates $S$	1
Maximum iterations	1000
Samples per draw $B$	10, 50
Noise scale $\sigma$	$1 \times 10^{-3}$
Initial learning rate $\alpha_0$	$1 \times 10^{-1}$
Minimum learning rate	$1 \times 10^{-4}$
Momentum coefficient	0.9
Update rule	sign-based descent

towards learning the inverse mapping for speaker identity across the entire generation pipeline.

**D.2.4 Details of Fixed Text.** For training the inverse model, we employ fixed text sets in both English and Chinese. The English text set consists of the following utterances: “Can you hear my voice clearly now”, “Hello Google, Hi Siri, Hey Bixby”, and “Up down left right start now again”. For training Chinese inverse model, text set consists of the following utterances: “Hello Google, Hi Siri, Hey Bixby” and “Ni hao ya, Gu ge, bang wo yi xia”.

Among these, we use “Hello Google, Hi Siri, Hey Bixby” as the primary fixed text for reporting the inverse model training results, as it is shared across both languages. We observe that restricting the inverse model to a fixed text does not introduce a noticeable change in the overall attack behavior or performance trends. This indicates that the proposed attack is largely insensitive to the specific choice of fixed text.

**D.2.5 Details of Audio-NES.** Algorithm 1 describes the Audio-NES attack, which performs score-based optimization directly in the waveform space. The attacker interacts with the target speaker recognition system  $T$  exclusively through a score-only black-box oracle  $\text{QUERY}(\cdot)$ , which returns a similarity score between a query audio and the victim utterance. No access to internal representations, model parameters, or gradients of  $T$  is assumed.

The optimization variable is a waveform  $\text{aud} \in \mathbb{R}^{48000}$ , corresponding to 3 seconds of audio sampled at 16 kHz. At each iteration, Audio-NES estimates a gradient direction using Natural Evolution Strategies (NES) with  $B$  random perturbations. The gradient estimate is then used to update the waveform via sign-based descent.

The total query budget  $Q$  is determined by the product of the number of perturbation samples per iteration  $B$  and the maximum number of iterations:  $Q = B \times \text{txtttmax\_iter}$ . Unless stated otherwise, all reported Audio-NES results correspond to the configuration that achieves the best attack performance among the tested values of  $B$  (cf. Table 11). If multiple configurations yield comparable performance, we report the result with the smaller total query count.

**D.2.6 Details of Latent-NES.** Algorithm 2 presents the Latent-NES attack, which operates in a low-dimensional latent space and synthesizes attack audio via an inverse decoder. This algorithm is used

---

**Algorithm 1** Audio-NES

---

**Input:** target oracle  $\text{QUERY}(T, \cdot, \cdot)$ , victim utterance  $\text{aud}_{\text{vic}} \in \mathcal{A}$ , query budget  $Q$ , threshold  $\tau$ , step size  $\alpha$ , noise scale  $\sigma$ , samples per draw  $B$

**Output:** adversarial audio  $\text{aud}^*$  (or best found)

```

1: initialize  $\text{aud}_0 \sim \mathcal{N}(0, I_{48000})$  and clip to  $[-1, 1]$ 
2: for  $t = 1, 2, \dots$  while cumulative queries  $\leq Q$  do
3:   Sample  $\epsilon_1, \dots, \epsilon_N \sim \mathcal{N}(0, I)$  ▷ optionally antithetic
4:   for  $i = 1$  to  $B$  do
5:      $\text{aud}_i \leftarrow \text{clip}(\text{aud}_{t-1} + \sigma \epsilon_i)$ 
6:      $s_i \leftarrow \text{QUERY}(T, \text{aud}_i, \text{aud}_{\text{vic}})$ 
7:      $\ell_i \leftarrow 1 - s_i$ 
8:   end for
9:    $\hat{g} \leftarrow \frac{1}{B\sigma} \sum_{i=1}^B \ell_i \epsilon_i$ 
10:   $\text{aud}_t \leftarrow \text{clip}(\text{aud}_{t-1} - \alpha \cdot \text{sign}(\hat{g}))$ 
11:   $s \leftarrow \text{QUERY}(T, \text{aud}_t, \text{aud}_{\text{vic}})$ ;  $\ell \leftarrow 1 - s$ 
12:  if  $\ell \leq \tau$  then
13:    return  $\text{aud}_t$ 
14:  end if
15: end for
16: return best found  $\text{aud}^*$ 

```

---

for both *YourTTS-NES* and *Ours-NES*, differing only in the choice of the inverse model  $G$ . The optimization procedure itself remains identical across these two instantiations.

Latent-NES optimizes a latent vector  $z$  constrained to the unit hypersphere  $S^D$ . At each iteration, spherical NES perturbations are applied to  $z$ , and each perturbed latent vector is decoded into audio using  $G(z, \text{Text})$ , where the text input  $\text{Text}$  is fixed throughout the attack. The resulting audio samples are evaluated via the same score-only black-box oracle  $\text{QUERY}(\cdot)$  as in Audio-NES.

As in the audio-space case, the total query budget is expressed as  $Q = B \times \text{max\_iter}$  where  $B$  denotes the number of NES samples per iteration. All Latent-NES results reported in the main paper are obtained using the configuration that yields the best attack performance among different values of  $B$  (see Table 12). When multiple configurations achieve similar success, the one with fewer queries is selected.

We emphasize that, despite operating in a latent space, Latent-NES strictly adheres to the same score-based black-box threat model as Audio-NES. The attacker never observes speaker embeddings or internal features of the target system and relies solely on similarity scores returned by the oracle.

**D.2.7 Construction of  $\delta$ -Orthogonal Voice Set.(Ours-SP).** To construct the  $\delta$ -OVS, we used VoxCeleb1 [50] and trainset as datasets. First, we performed pre-processing to extract feature vectors for all utterances in the dataset using the speaker recognition model used as the speaker encoder of YourTTS. After that, we constructed a set satisfying the  $\delta$ -OVS constraint in Definition 1, where  $\delta \approx 0.2$  and the OVS size is 50.

**D.2.8 Details of Audio-GD.** Audio-GD is a white-box baseline that generates impersonation audio by directly optimizing the waveform in the audio domain. Given a target speaker embedding  $t$ , the attack iteratively updates an audio signal  $\tilde{\mathbf{u}}$  via gradient descent to minimize the cosine distance between the extracted embedding

**Algorithm 2** Latent-NES (for YourTTS, Ours-NES)

---

**Input:** target oracle  $\text{QUERY}(T, \cdot, \cdot)$ , inverse decoder  $G : \mathbb{R}^D \times \mathcal{T} \rightarrow \mathcal{A}$ , victim utterance  $\text{aud}_{\text{vic}}$ , fixed text  $\text{Text} \in \mathcal{T}$ , query budget  $Q$ , threshold  $\tau$ , step size  $\alpha$ , noise scale  $\sigma$ , samples per draw  $B$

**Output:** latent  $z^*$  and audio  $\text{aud}^* = G(z^*, \text{Text})$  (or best found)

- 1: initialize  $z_0 \sim \mathcal{N}(0, I_D)$  and normalize  $z_0 \leftarrow z_0 / \|z_0\|_2$
- 2: **for**  $t = 1, 2, \dots$  while cumulative queries  $\leq Q$  **do**
- 3:   Sample  $\epsilon_1, \dots, \epsilon_B \sim \mathcal{B}(0, I_D)$
- 4:   **for**  $i = 1$  to  $B$  **do**
- 5:      $\tilde{z}_i \leftarrow \frac{z_{t-1} + \sigma \epsilon_i}{\|z_{t-1} + \sigma \epsilon_i\|_2}$
- 6:      $\text{aud}_i \leftarrow G(\tilde{z}_i, \text{Text})$
- 7:      $s_i \leftarrow \text{QUERY}(T, \text{aud}_i, \text{aud}_{\text{vic}})$
- 8:      $\ell_i \leftarrow 1 - s_i$
- 9:   **end for**
- 10:    $\hat{g} \leftarrow \frac{1}{B\sigma} \sum_{i=1}^B \ell_i \epsilon_i$
- 11:    $z_t \leftarrow \frac{z_{t-1} - \alpha \hat{g}}{\|z_{t-1} - \alpha \hat{g}\|_2}$
- 12:    $\text{aud}_t \leftarrow G(z_t, \text{Text})$
- 13:    $s \leftarrow \text{QUERY}(T, \text{aud}_t, \text{aud}_{\text{vic}})$ ;    $\ell \leftarrow 1 - s$
- 14:   **if**  $\ell \leq \tau$  **then**
- 15:     **return**  $z_t, \text{aud}_t$
- 16:   **end if**
- 17: **end for**
- 18: **return** best found  $z^*$  and  $\text{aud}^* = G(z^*, \text{Text})$

---

**Table 12: Hyperparameters for latent(spherical) NES. (for Ours-NES, YourTTS-NES)**

Hyperparameter	Value
Search variable	latent vector $z \in \mathbb{S}^D$
Initialization	$\mathcal{N}(0, I_D) + \ell_2$ normalization
Candidate pool size $C$	100
Selected candidates $S$	1
Maximum iterations	1000
Samples per draw $B$	10, 50
Noise scale $\sigma$	5.0
Initial learning rate $\alpha_0$	$5 \times 10^{-2}$
Minimum learning rate	$1 \times 10^{-6}$
Momentum coefficient	0.9
Update rule	spherical gradient descent

$F(\mathbf{v})$  and  $t$ . Gradients are computed through the speaker recognition model and applied to the audio samples until convergence or a predefined iteration limit. This approach serves as a tool for inversion via optimization in the high-dimensional audio space, without relying on generative priors or inverse models.

### D.3 Model Configurations

Table 13 summarizes the speaker recognition models used in our study, categorized into two groups: target models ( $T_1$ – $T_5$ ) and attacker-side local models ( $L_{\text{SV2TTS}}$ ,  $L_{\text{Vox}}$ , and  $L_{\text{Ours}}$ ). The target models employ a diverse range of architectures and size—including RedimNet [81], SimAMResNet [62], and Titanet [39]—trained on either

**Algorithm 3** Attack Audio Generation via Gradient Descent (Audio-GD)

---

**Input:** SR feature extractor  $F : \mathcal{A} \rightarrow \mathbb{S}^{d-1}$ , original audio  $\text{aud}_{\text{orig}} \in \mathcal{A}$ , target embedding  $x \in \mathbb{S}^{d-1}$ , learning rate  $\eta$ , max iterations  $K_{\text{max}}$ , optional convergence threshold  $\epsilon$

**Output:** Optimized attack audio  $\tilde{a} \in \mathcal{A}$

- 1: Initialize audio:  $\tilde{a} \leftarrow \tilde{a}_0$
- 2: Initialize step counter:  $K \leftarrow 0$
- 3: Initialize previous loss:  $\mathcal{L}_{\text{prev}} \leftarrow \infty$
- 4: **repeat**
- 5:   Compute current embedding:  $\tilde{x} \leftarrow F(\tilde{a})$
- 6:   Compute loss:  $\mathcal{L}_{\text{now}} \leftarrow 1 - \frac{\langle \tilde{x}, x \rangle}{\|\tilde{x}\| \|x\|}$
- 7:   Compute gradient of loss w.r.t. audio input:  $\nabla_{\tilde{a}} \mathcal{L}_{\text{now}}$
- 8:   Update audio signal:  $\tilde{a} \leftarrow \tilde{a} - \eta \cdot \nabla_{\tilde{a}} \mathcal{L}_{\text{now}}$
- 9:    $K \leftarrow K + 1$
- 10:   Check for convergence  $\Delta \mathcal{L} = |\mathcal{L}_{\text{prev}} - \mathcal{L}_{\text{now}}|$
- 11:    $\mathcal{L}_{\text{prev}} \leftarrow \mathcal{L}_{\text{now}}$
- 12: **until**  $K \geq K_{\text{max}}$  or  $\Delta \mathcal{L} \leq \epsilon$
- 13: **return** Optimized audio  $\tilde{a}$

---

VoxBlink2 [42] or large-scale aggregated corpora such as VoxCeleb1 [50], VoxCeleb2 [17], Fisher [18], Switchboard [24], LibriSpeech [63]. This variation ensures coverage of a wide spectrum of real-world systems in our evaluation.

On the attacker side, the local models are configured to reflect realistic black-box constraints, with both architectural and training data separation from the target models. Specifically,  $L_{\text{SV2TTS}}$  utilizes a GE2E [72]-based speaker encoder,  $L_{\text{Vox}}$  adopts the RawNet3 [33] architecture optimized for end-to-end verification, and  $L_{\text{Ours}}$  employs a hybrid structure integrating heuristic attention and ASP [27] modules. For simplicity,  $L_{\text{Ours}}$  is referred to as  $L$  throughout the main text.

In addition to model architecture and training data, the table also includes key performance metrics: Equal error rate (EER), minimum detection cost function (minDCF), and their respective decision thresholds ( $\tau_E$  and  $\tau_M$  for minDCF); all evaluated on the VoxCeleb1 test set.

### D.4 Additional Experiments: Original FakeBob

For the baseline comparison presented in Tab. 1, we reproduced the FakeBob [9] attack following the methodology provided in SpeakerGuard’s [11] official codebase. The attack was configured to perform targeted impersonation against our targeted systems acting as speaker verification systems ( $T_1$ – $T_5$ ). Consistent with FakeBob’s requirements, each attack trial commenced with an initial seed utterance and aimed to iteratively refine it by querying the target system’s scores until it surpassed the pre-determined EER decision threshold. This iterative optimization process was capped at a maximum of 1000 iterations. Within each iteration, the gradient direction was estimated by sampling 50 perturbation samples, generated using Gaussian noise with a standard deviation of 0.001, and querying their scores from the target system; these queries were processed efficiently in a single batch. Updates were performed using a momentum of 0.9 and an adaptive learning rate strategy.

**Table 13: Specifications and performance of the speaker recognition models used in this paper, including the target models ( $T_1$ – $T_5$ ) and the attacker’s local models ( $L_{SV2TTS}$ ,  $L_{Vox}$ , and  $L_{Ours}$ ). Note that ‘ $L_{Ours}$ ’ is referred to as ‘ $L$ ’ in the main paper. Performance is evaluated using EER, minDCF, and the corresponding thresholds  $\tau_E$  and  $\tau_M$  on the VoxCeleb1 test set. For the Chinese speaker recognition models ( $C_1$ ,  $C_2$ ) and the local model ( $L_{CN}$ ), performance is evaluated on the CN-Celeb test set.**

Index	Architecture	Trainset	EER(%)	minDCF	$\tau_E$	$\tau_M$
$T_1$	Redim-S	VoxBlink2	1.54	0.1415	0.6605	0.5518
$T_2$	Redim-M	VoxBlink2	1.31	0.1003	0.6624	0.5437
$T_3$	SimAMResNet34	VoxBlink2	1.16	0.1039	0.6258	0.5060
$T_4$	SimAMResNet100	VoxBlink2	0.76	0.0767	0.6137	0.4932
$T_5$	Titanet-L	VoxCeleb1,2, Fisher, Switchboard, LibriSpeech	0.82	0.1353	0.6654	0.5215
$C_1$	CAM++	N/A	4.70	0.3120	0.7064	0.4817
$C_2$	ERE2Net	N/A	2.79	0.1779	0.6350	0.4617
$L_{SV2TTS}$	GE2E	VoxCeleb1,2	8.28	0.6810	0.3232	0.2100
$L_{Vox}$	Rawnet3	VoxCeleb1,2	0.83	0.1111	0.6619	0.5236
$L_{CN}$	ResNet34	CNCeleb	7.54	0.4575	0.7349	0.5043
$L_{Ours}$	H/ASP	VoxCeleb1,2	1.18	0.1339	0.5778	0.4667

**Table 14: FakeBob attack performance against target models  $T_1$ – $T_5$ , showing attack successes (out of 50 trials) and the number of queries required solely for the attack generation phase (excluding threshold estimation).**

Methods	$T_1$	$T_2$	$T_3$	$T_4$	$T_5$
Ours	46/50	44/50	37/50	36/50	36/50
FakeBob	43/50	43/50	32/50	29/50	34/50
# of Queries	$\approx 14233$	$\approx 14067$	$\approx 14073$	$\approx 13181$	$\approx 11552$

The learning rate started at 0.001 and was halved if no score improvement was observed for 5 consecutive iterations, down to a minimum of  $1e-6$ . Furthermore, early stopping was enabled, terminating the process if the best achieved score did not change for 100 iterations. Other configuration parameters included using an  $\epsilon$  value of 0.002 and processing the samples individually. Crucially, the query counts reported in Table 14 encompass only those consumed during this iterative attack generation phase, excluding any potentially required for initial threshold estimation, thereby facilitating a direct comparison with the query efficiency of our proposed method.

## E In-depth Analysis of Ours-SP

In this section, we provide a detailed analysis of our attack. We begin by outlining the overall attack pipeline and discussing specific errors or gaps encountered at each stage of the process. Then we analyze how these issues influenced the overall success rate of the attack. Furthermore, we present an evaluation of black-box transfer settings by assessing their success rates against target models that were not explicitly used during the attack generation phase.

We present a score-based non-adaptive impersonation attack within the speaker recognition domain by generalizing the framework originally established by [36] for attacking face recognition systems. Let  $T : \mathcal{B} \rightarrow [-1, 1]$  be a target black-box biometric recognition system with an enrolled biometric datum  $e$ . The attacker

has a local feature extractor  $F_L : \mathcal{B} \rightarrow \mathbb{S}^{d-1}$  and a corresponding inverse model  $F_L^{-1} : \mathbb{S}^{d-1} \rightarrow \mathcal{B}$ , both constructed independently of  $T$ . The impersonation attack consists of the following steps:

- (1) **Feature Space Reduction via Target Queries.** The attacker queries  $T$  with a local set of samples  $(b_1, \dots, b_n)$  and collects corresponding scores  $s_i = T(b_i)$ . Assuming that models trained for the same task behave similarly, we expect the local extractor to align well with the target system in similarity scores. Based on this assumption, we approximate  $s_i \approx \langle F_L(b_i), F_L(e) \rangle$ .
- (2) **Solving Linear System for the Feature Vector.** Treating  $F_L(b_i)$  as known row vectors, setting  $A$  such that its  $i$ -th row is  $s_i = F_L(b_i)$ , the system can be expressed as  $Ax = y$ , where  $y = (s_1, \dots, s_n)^T$ , and solved via least squares to approximate the (local) feature vector of the enrolled identity  $\hat{x} \approx F_L(e)$ . To ensure numerical stability, a well-conditioned query set is crucial. We define:
 

DEFINITION 1 ( $\delta$ -ORTHOGONAL BIOMETRIC SET ( $\delta$ -OBS)). Given  $F : \mathcal{B} \rightarrow \mathbb{S}^{d-1}$ , a set  $O = \{o_1, \dots, o_m\}$  is a  $\delta$ -OBS if  $|\langle F(o_i), F(o_j) \rangle| \leq \delta$  for all  $i \neq j$ .
- (3) **Pre-image Reconstruction.** Using the solved feature vector  $\hat{x}$ , the attacker generates an input sample  $b'$  such that  $F_L(b') \approx \hat{x}$ , in order to satisfy  $T(b') > \tau$ , where  $\tau$  is the acceptance threshold. In the SR domain, this step requires a feasible  $F_L^{-1}$  model inverting  $\hat{x}$  into audio.

### E.1 Error Analysis of the Attack Pipeline

The flow of our attack is illustrated in Figure 10, and the detailed algorithm is described in Figure 9. The attack consists of three main steps: (1) reducing the problem from the target model  $T$  to a local feature space, (2) solving for the feature representation in this local space, and (3) synthesizing a biometric sample  $b'$  that can successfully impersonate the target  $T$ . Specifically, lines 1–4 in the algorithm correspond to (Step 1), line 5 implements (Step 2), and line 6 executes (Step 3).

<b>Non-Adaptive Black-Box Impersonation Attack (Ours-SP)</b>	
<b>Inputs:</b>	
<ul style="list-style-type: none"> <li>• The black-box access target SRS <math>T : \mathcal{A} \rightarrow [-1, 1]</math> with enrolled voice aud.</li> <li>• The local SR feature extractor <math>F : \mathcal{A} \rightarrow \mathbb{S}^{d-1}</math> and its inverse model <math>F^{-1} : \mathbb{S}^{d-1} \rightarrow \mathcal{A}</math>.</li> <li>• The local voice dataset <math>\mathcal{D}</math> where <math> \mathcal{D}  = n</math> and <math>n \in \mathbb{N}</math>.</li> <li>• The pre-defined parameter <math>\delta \in [-1, 1]</math> and <math>m \in \mathbb{N}</math>.</li> </ul>	
<b>Output:</b> $\widehat{\text{aud}}$	
<b>Pre-processing (<math>\delta</math>-OVS generation):</b>	
<ol style="list-style-type: none"> <li>1: Set <math>f_i \leftarrow F(\mathcal{D}_i)</math> for <math>\forall i \in [n]</math></li> <li>2: Find a set of indices <math>I = \{I_1, \dots, I_m\} \subseteq [n]</math> of size <math>m</math> such that <math>\max_{j,k \in I}  \langle f_j, f_k \rangle  \leq \delta</math></li> <li>3: <math>O \leftarrow \{o_i = \mathcal{D}_{I_i}   i \in [m]\}</math></li> </ol>	
<b>Algorithm:</b>	
<ol style="list-style-type: none"> <li>1: Query and set <math>s_i \leftarrow T(o_i)</math> for <math>\forall i \in [m]</math>.</li> <li>2: Set <math>s \in [-1, 1]^m</math>, whose <math>i</math>'th element is <math>s_i</math> for <math>\forall i \in [m]</math>.</li> <li>3: Extract and set <math>A_i \leftarrow F(o_i)</math> for <math>\forall i \in [m]</math>.</li> <li>4: Set <math>A \leftarrow [A_1, \dots, A_m]^T</math>.</li> <li>5: <math>r \leftarrow A^\dagger s</math></li> <li>6: <math>\widehat{\text{aud}} \leftarrow F^{-1}(r/\ r\ )</math></li> <li>7: <b>Return</b> <math>\widehat{\text{aud}}</math>.</li> </ol>	

**Figure 9: Algorithm for Non-Adaptive Black-box Impersonation Attack on an SRS.**

The overall attack pipeline comprises three key stages whose effectiveness depends on managing and mitigating the cumulative impact of errors introduced throughout the process. While these errors do not propagate in a purely additive manner, we decompose them step-by-step to better understand which components most significantly influence attack success and where improvements could yield the greatest benefit. This breakdown offers a more comprehensive view into the attack dynamics, highlighting how different sources of error interplay to shape the final outcome.

In (Step 1), discrepancies arise between the local and target models due to imperfect alignment of their feature space (more accurately, similarity scores), which can distort the recovered objective. (Step 2) introduces numerical inaccuracies during the pseudo-inversion process used to estimate the enrolled feature vector. (Step 3) involves synthesizing an audio sample from the recovered feature such that it both conforms to the input requirements of the target model and preserves alignment with the intended feature representation.

## E.2 Model Discrepancy

Table 15 presents the mean and standard deviation of the absolute differences in cosine similarity scores between each local model and the five target models ( $T_1$ – $T_5$ ), evaluated over all verification pairs in the VoxCeleb1 test set. Among the three local models,  $L_{SV2TTS}$  exhibits significantly larger score discrepancies, with mean

**Table 15: Statistical summary of score discrepancies between local and target models ( $T_1$ – $T_5$ ) on the VoxCeleb1 test set. Each entry reports the mean and std. of the absolute differences in cosine similarity scores across all pairs.**

$T$	$L_{SV2TTS}$	$L_{Vox}$	$L_{Ours}$
$T_1$	$0.3304 \pm 0.2017$	$0.0617 \pm 0.0479$	$0.0741 \pm 0.0582$
$T_2$	$0.3305 \pm 0.2076$	$0.0588 \pm 0.0461$	$0.0757 \pm 0.0594$
$T_3$	$0.2999 \pm 0.2143$	$0.0675 \pm 0.0517$	$0.0691 \pm 0.0523$
$T_4$	$0.2935 \pm 0.2248$	$0.0722 \pm 0.0528$	$0.0760 \pm 0.0548$
$T_5$	$0.3461 \pm 0.2191$	$0.0484 \pm 0.0387$	$0.0804 \pm 0.0664$

**Table 16: Cosine similarity between the recovered feature  $x'$  and original feature  $x$  using a fixed pseudo-inversion matrix  $A$  constructed from  $L_{Ours}$ . The condition number of  $A$  is  $\text{cond}(A) = 3.8692$  and remains constant across all rows.**

$F$	$\langle x', x \rangle$
$T_1$	0.3134
$T_2$	0.3112
$T_3$	0.3114
$T_4$	0.3004
$T_5$	0.3151

deviations exceeding 0.29 in all cases. In contrast,  $L_{Vox}$  and  $L_{Ours}$  demonstrate much smaller deviations than typically 0.08, indicating closer alignment with the scoring behavior of the target models.

This observation is further supported by the scatter plots shown in Figure 11, which visualize the relationship between similarity scores produced by local models and their corresponding target models for all test pairs. Ideally, if a local model accurately approximates the target model scoring behavior, the points should be along the identity line ( $y = x$ ), and the correlation between the two scores should be high. However, the scatter plots for  $L_{SV2TTS}$  reveal a large dispersion from the identity line, indicating low agreement in absolute score values. Furthermore, Pearson’s correlation coefficients  $R$  which quantify the linear agreement between the local and target model scores are consistently lower for  $L_{SV2TTS}$  compared to the other two models. This suggests that the absolute scores are not only misaligned, but also that the relative ranking or trend of scores is poorly preserved.

In contrast, both  $L_{Vox}$  and  $L_{Ours}$  achieve higher  $R$  values in all target models, indicating that they better preserve the similarity of test pairs. This is consistent with their lower score discrepancies and visually tighter clustering around the diagonal in the scatter plots. Together, these results suggest that  $L_{Vox}$  and  $L_{Ours}$  offer a more faithful approximation of the behavior of the target model in terms of the alignment of the absolute scores. This is critical for the effectiveness of (Step 1) in the attack pipeline.

## E.3 Numerical Error in Pseudo-Inverse

We now analyze the numerical stability of the pseudo-inversion step in our pipeline, where a linear system of the form  $Ax = y$  is solved to recover the enrolled feature vector  $x$  from a score vector  $y$  and a matrix  $A$  constructed from local features. In practice, the score

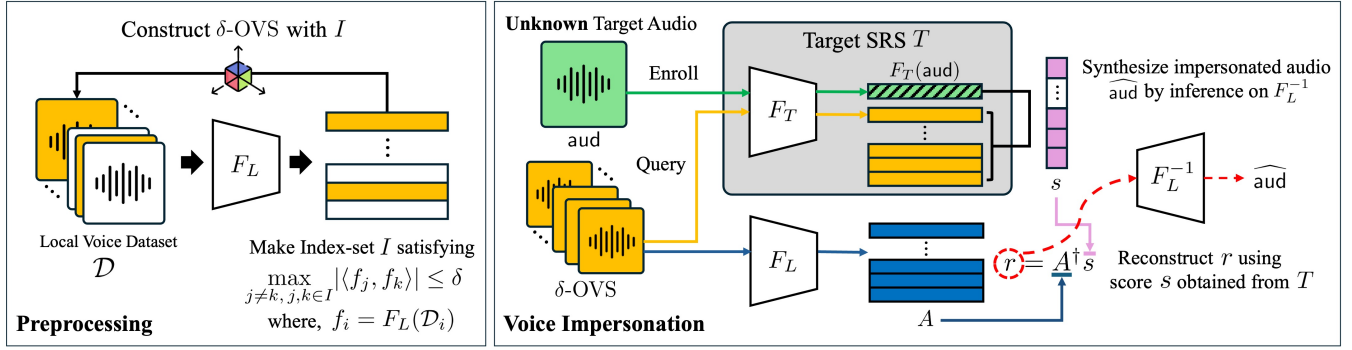


Figure 10: Flow diagram of the proposed Non-Adaptive Speaker Impersonation Attack applied to SRSs (Ours-SP). Key stages include pre-processing for  $\delta$ -OVS generation, querying the target SRS, and synthesizing the impersonation audio. Note that the attacker cannot directly access the black-box target  $T$  (and  $F_T$ ). The local models ( $F_L$  and  $F_L^{-1}$ ) are used as surrogate for the attack.

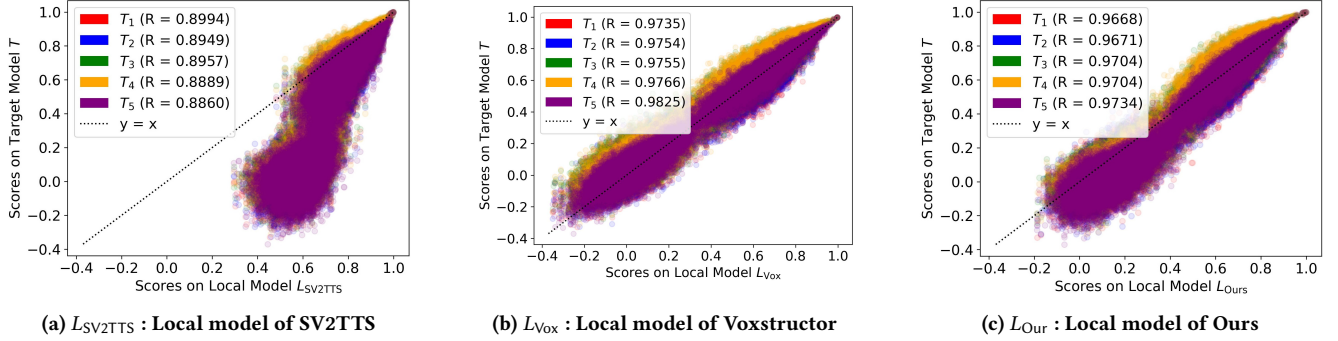


Figure 11: Scatter plots of the cosine similarity values output by local models for all pairs from the Voxceleb1 testset;  $R$  is the correlation coefficient between scores output by  $L$  different target models ( $T_1$ - $T_5$ ).

vector may contain small perturbations, i.e.,  $y' = y + \epsilon$ , resulting in an approximate solution  $x'$  upon inversion. The propagation of such perturbations through the pseudo-inversion is governed by the condition number of  $A$ , defined as

$$\text{cond}(A) = \|A\| \cdot \|A^\dagger\|,$$

where  $A^\dagger$  is the Moore–Penrose pseudo-inverse. This yields the classical upper bound on the relative error:

$$\frac{\|x' - x\|}{\|x\|} \leq \text{cond}(A) \cdot \frac{\|y' - y\|}{\|y\|}.$$

A large condition number implies that even small perturbations in the input can lead to significant deviations in the recovered feature vector, indicating poor numerical stability of the inversion.

In our setting, the matrix  $A$  is constructed once from features generated by the local model  $L_{Ours}$  and remains fixed for all evaluations. Consequently, the condition number depends solely on the local model and is invariant across different score sources. For the local model used in our attack, we empirically find  $\text{cond}(A) = 3.8692$ .

We restrict this analysis to  $L_{Ours}$ , as preliminary experiments have shown that other baselines—such as SV2TTS and Voxstructor—fail to preserve identity consistency across embeddings or high model discrepancy. These models exhibit semantically inconsistent

behavior, rendering pseudo-inversion unreliable regardless of its numerical stability.

To assess how the mismatch between score source and the local feature space affects the recovered vector, we compute the cosine similarity between the recovered feature  $x'$  and the ground truth feature  $x$  across different target models. Each rows reflect black-box cases where  $y$  is computed using each of the target models  $T_1$ - $T_5$ .

#### E.4 Implicit Noise Purification Effect

In practice, the recovered feature vectors from the pseudo-inversion step inevitably contain noise, and directly using these noisy features can result in unsuccessful attacks in some cases. However, we observe an implicit noise purification effect when the recovered features are passed through the inverse model. Table 17 demonstrates this effect under both synthetic noise (added with increasing angular perturbations) and real attack noise.

Although we do not offer a complete theoretical account of this phenomenon, it can be intuitively understood. The inverse models, as well as the foundation model (YourTTS), is trained to produce outputs corresponding to clean feature vectors extracted from actual speech data. In contrast, the recovered vectors are corrupted and therefore unlikely to lie on the same distribution as

**Table 17: Analysis of ID-constraint robustness under noise with random noise (10° to 40°).**

Feat.	YourTTS	YourTTS + $L_{IC}$	YourTTS + $L_{IC}$ + $L_{SC}$
Org.	0.4011 ± 0.0919	0.9026 ± 0.0197	0.8390 ± 0.0285
+10°	0.3959 ± 0.0922	0.8978 ± 0.0204	0.8349 ± 0.0291
+20°	0.3804 ± 0.0925	0.8832 ± 0.0225	0.8220 ± 0.0309
+30°	0.3556 ± 0.0937	0.8559 ± 0.0267	0.7973 ± 0.0346
+40°	0.3213 ± 0.0949	0.8114 ± 0.0345	0.7555 ± 0.0418

genuine features. As a result, the trained inverse model tends to map these noisy inputs toward outputs that are more consistent with the training distribution—that is, it effectively "denoises" the input by projecting it onto the learned feature manifold.

This behavior is in line with the general observation that deep learning models often demonstrate robustness to distribution shifts, especially when the test samples are mapped to high-density regions of the training distribution. In our context, this manifests as a denoising effect that increases identity-consistency and improves the effectiveness of the attack, even under considerable input perturbations.

We believe that further investigation into this implicit purification effect—both in theoretical and empirical terms—would be a promising direction for future research, particularly in understanding how neural models implicitly regularize noisy or out-of-distribution representations.

## F Discussion

### F.1 About DeepFake Detection

A pertinent question arising from any method generating synthetic or manipulated voice audio is whether existing defense mechanisms, particularly deepfake detectors, can identify such samples. Our attack generates audio that, while mimicking the target speaker’s voice identity extracted from an embedding, constitutes speech content potentially never uttered by the actual speaker in that sequence. This places the generated audio in the realm of synthetic speech, which deepfake detection models aim to expose.

To investigate this, we evaluated the audio samples generated by our attack method using an anti-spoofing model. The deepfake detection system used in our evaluation is based on the framework and pre-trained components from the Self-Supervised Learning (SSL)-based anti-spoofing approach. Specifically, the detector [68] utilizes a powerful pre-trained SSL audio model as a feature extractor. On top of these SSL features, an AASIST back-end classifier is applied to generate prediction scores for the anti-spoofing task. The model is trained using the standard ASVspoof 2019 Logical Access (LA) [69] dataset, which includes a variety of spoofed audio types relevant to deepfake scenarios. For consistency and reproducibility, we utilize the publicly available pre-trained weights associated with this architecture provided by the authors.<sup>2</sup>

This model outputs a score reflecting the likelihood that an input audio sample is spoofed. Classification decisions are based on comparing this score against a predefined threshold,  $\tau_{DF}$ . We adopted the standard practice of setting  $\tau_{DF}$  to the value corresponding

<sup>2</sup>[https://github.com/TakHemlata/SSL\\_Anti-spoofing](https://github.com/TakHemlata/SSL_Anti-spoofing)

**Table 18: Results (%) of the Deepfake detection [68] of audio samples classified as ‘Spoof’ or ‘Bonafide’ for genuine VoxCeleb1 audio, audio generated by YourTTS, and audio generated by our proposed method (‘Ours’).**

Decision	VoxCeleb1 Testset	YourTTS	Ours
Spoof	8.05%	55.90%	12.55%
Bonafide	91.95%	44.10%	87.45%

to the Equal Error Rate (EER) operating point, determined from publicly available performance results for this model configuration. According to these results, the detector achieves an EER of 2.85% on the ASVspoof 2021 deepfake (DF) track evaluation set [82]. Input audio samples producing scores exceeding this EER threshold were consequently classified as deepfakes.

We conducted a comparative test using three distinct sets of audio derived from the VoxCeleb1 testset identities: (1) original, genuine speech samples from VoxCeleb1; (2) synthetic samples generated by the baseline YourTTS [8] using the corresponding speaker embeddings; and (3) synthetic samples generated by our proposed attack method. The deepfake detector was tasked with assessing the authenticity or ‘spoofiness’ of samples from each set.

The results in Table 18 revealed a clear trend in the detector’s assessment. Audio generated by YourTTS was most frequently identified as spoofed or assigned the highest spoofiness scores. Genuine VoxCeleb1 audio, as expected, received the lowest spoofiness scores. Crucially, the audio generated by our method received scores indicating significantly lower spoofiness compared to YourTTS, placing it much closer to the distribution of genuine audio. This suggests that our generated samples are considerably harder for this type of detector to distinguish from real speech compared to those from the YourTTS synthesis pipeline.

We attribute this increased resilience against detection to a potentially advantageous side-effect of our training strategy, specifically the fine-tuning of the vocoder module. Many deepfake detection systems are trained on large datasets containing audio generated by commonly used, pre-trained vocoders. Consequently, they learn to identify characteristic artifacts or patterns inherent in the outputs of these standard vocoders. Our method, however, incorporates fine-tuning of vocoder parameters as part of its training process. We hypothesize that this fine-tuning process alters the typical acoustic artifacts produced by the baseline vocoder, effectively removing or modifying the very cues the deepfake detector relies upon. As a result, the audio produced by our fine-tuned system lacks the expected signs of synthesis, leading to lower spoofiness scores. This finding underscores that the specific mechanism of synthetic speech generation, particularly modifications to the vocoder, can significantly impact detectability, posing challenges for current artifact-based deepfake detection approaches and highlighting the need for detection methods robust to such variations.

### F.2 Cross-Lingual Attack Evaluation

Our primary evaluations focused on target speaker verification models predominantly trained on English datasets such as Voxceleb1,2 and VoxBlink2. A natural question arises regarding the generalizability of our proposed attack across languages with differing

**Table 19: Cross-lingual attack performance against a ResNet34 model trained on CNCeleb. Thresholds and baseline metrics were derived using the ASR was computed under these thresholds.**

Evaluation		Threshold	ASR(%)	FRR(%)
EER	7.73	0.4246	60.24	(= EER)
minDCF	0.6428	0.6484	0.06	60.26

acoustic and linguistic properties. This is especially pertinent given that prior studies in areas like speech anti-spoofing have shown performance degradation when training and evaluation languages differ [43]. To explore this, we conducted an auxiliary experiment targeting a speaker verification model trained on a linguistically distinct language: Chinese.

We chose Chinese due to the availability of large-scale datasets like CNCeleb [23], as well as the presence of pre-trained models such as those provided by the WeSpeaker toolkit [73]<sup>3</sup>. Furthermore, the substantial linguistic distance between Chinese and English—given differences in phonology, tonal structure, and syntax—makes this a rigorous test case for assessing the cross-lingual transferability of our attack. This experiment was not the central focus of our study but serves as an exploratory evaluation of the language-agnostic potential of targeting speaker embeddings.

The target system in this experiment was a ResNet34-based speaker verification model trained exclusively on the CNCeleb dataset. CNCeleb contains a diverse range of Chinese conversational speech across various conditions, making it a robust benchmark for Chinese SV research.

To evaluate our attack under mismatched linguistic conditions, we assessed this Chinese-trained model using the English VoxCeleb1 testset. Although unconventional for standard SV benchmarking, this cross-lingual evaluation setup allowed us to (1) derive consistent operating thresholds for evaluation, and (2) simulate realistic mismatched-language attack scenarios where attacker queries originate from a different language domain.

We first computed the baseline performance of the model on the VoxCeleb1 testset to determine operating points. The evaluation yielded an Equal Error Rate (EER) of 7.73% at a threshold of 0.4246, and a minimum Detection Cost Function (minDCF) of 0.6428 at a threshold of 0.6484.

Using the attack methodology Ours-SP, we evaluated the success of our attack under these two operating thresholds. At the EER threshold (0.4246), the attack achieved a success rate (ASR) of 60.24%, indicating a clear ability to deceive the system despite the mismatch in language between model training and attack data. This result suggests that our attack, which targets the speaker embedding space, is capable of exploiting voice characteristics that are not strictly language-dependent.

In contrast, when evaluated under the stricter minDCF threshold of 0.6484—which corresponds to a high-precision, low false acceptance setting—the ASR dropped to just 0.06%. This substantial drop is expected, as the minDCF threshold is tuned to reduce false positives and imposes a significantly stricter acceptance criterion. The corresponding False Rejection Rate (FRR) at this threshold was

60.26%, highlighting the challenge of evaluating a Chinese-trained model with out-of-domain English data.

Taken together, these findings provide two key insights. First, despite the linguistic mismatch, the attack exhibits a notable degree of cross-lingual transferability, successfully deceiving a Chinese-trained model using embeddings derived from English audio. This reinforces the idea that speaker embeddings capture speaker discriminative characteristics that are not strictly tied to linguistic content.

Second, the choice of operating threshold plays a critical role in determining the observed attack success. In this experiment, operating thresholds were derived from English VoxCeleb1 data, which constitutes an out-of-domain setting for the Chinese-trained target model  $L_{CN}$ . As a result, the minDCF threshold reflects a conservative operating point when applied to English inputs. In practice, speaker verification models trained on Chinese are typically calibrated using in-domain Chinese data (e.g., CNCeleb), and thresholds derived under such conditions would more accurately reflect the system’s operational vulnerability. This exploratory evaluation therefore highlights the sensitivity of cross-lingual attack assessment to threshold calibration, and motivates further investigation under fully in-domain settings.

### F.3 Limitation of Evaluation on Commercial APIs

SRSs have been actively deployed in practice through commercial APIs, and we fully acknowledge the value of evaluating against them. However, by early 2025, major providers such as Azure and Amazon had enforced strict Responsible AI policies, restricting hosted endpoints to prevent potential misuse. To ensure strict compliance with research ethics, we pursued official authorization for academic testing rather than bypassing these restrictions. We contacted smaller vendors—specifically PicoVoice in June 2025 and Phonexia in January 2026—but were unable to obtain the necessary approval.

Despite the lack of direct API access, we anticipate our findings to generalize to commercial systems. It is widely understood that modern commercial SRSs are built upon deep learning architectures [48] similar to those we evaluated. Furthermore, since our proposed attack is score-based, it does not require internal gradient access. Even if commercial APIs return only normalized confidence scores [4, 48], these can be effectively utilized for adversarial perturbations through inverse transformations or directly employed by NES [9, 86] (Natural Evolution Strategies)-based algorithms without loss of attack efficacy. To compensate for commercial-grade robustness, we adopted publicly available models provided by Alibaba’s 3D-Speaker research group and the NVIDIA model.

Received 20 February 2007; revised 12 March 2009; accepted 5 June 2009

<sup>3</sup><https://github.com/wenet-e2e/wespeaker>